Am J Cancer Res 2021;11(2):389-415
www.ajcr.us /ISSN:2156-6976/ajcr0122852

Original Article

CDCA8, targeted by MYBL2, promotes malignant progression and olaparib insensitivity in ovarian cancer

Gonghua Qi[1], Chenyi Zhang[1], Hanlin Ma[1,2], Yingwei Li[1,3], Jiali Peng[1,2], Jingying Chen[1], Beihua Kong[1,2]

[1]*Department of Obstetrics and Gynecology, Qilu Hospital, Shandong University, Jinan 250012, China;* [2]*Gynecologic Oncology Key Laboratory of Shandong Province, Qilu Hospital, Shandong University, Jinan 250012, China;* [3]*Institute of Oncology, School of Medicine, Shandong University, Jinan 250012, China*

Received September 22, 2020; Accepted December 7, 2020; Epub February 1, 2021; Published February 15, 2021

Abstract: Ovarian cancer is the most lethal gynecologic malignancy. Poly (ADP-ribose) polymerase inhibitors (PARPi) are effective in treating ovarian cancer. However, cancer cell insensitivity and resistance remain challenges. Determination of the exact chemoresistance mechanisms and potential targeted therapies is urgent. CDCA8 (cell division cycle associated 8) participates in the tumorigenesis of various cancers; however, the exact biological function of CDCA8 in ovarian cancer remains obscure. Here, we found that CDCA8 was overexpressed in ovarian cancer and that high expression of CDCA8 promoted the proliferation of ovarian cancer cells in vitro and in vivo. Moreover, silencing of CDCA8 sensitized ovarian cancer cells to olaparib and cisplatin by inducing G2/M arrest, accelerating apoptosis, increasing DNA damage and interfering with RAD51 accumulation in vitro. In addition, MYBL2 (MYB proto-oncogene-like 2), identified as an upstream transcription factor of CDCA8, was positively correlated with the expression level of CDCA8 in ovarian cancer. Finally, MYBL2 enhanced the aggressive characteristics of ovarian cancer cells by regulating CDCA8. In conclusion, high CDCA8 expression was involved in the tumorigenesis, aggressiveness and chemoresistance of ovarian cancer. CDCA8 silencing combined with olaparib treatment might lead to substantial progress in ovarian cancer targeted therapy.

Keywords: Ovarian cancer, CDCA8, olaparib, G2/M arrest, homologous recombination-mediated repair

Introduction

Ovarian cancer has been the leading cause of gynecologic malignancy-related death. Surgery followed by platinum/paclitaxel-based chemotherapy is still the standard therapy for ovarian cancer patients, although most patients develop resistance to platinum-based chemotherapy [1, 2], resulting in recurrence and death.

Recently, poly (ADP-ribose) polymerase inhibitors (PARPi) have emerged as effective ovarian cancer-targeted therapies, especially in patients with deleterious germline BRCA mutations [3-5]. Several PARPi (olaparib, rucaparib and niraparib) have been approved by the FDA as ovarian cancer therapies for maintenance and to prevent recurrence [1, 4]. PARPi perform their curative functions through synthetic lethality and PARP trapping [6]. While PARPi have displayed exact antitumor capacity, primary and acquired resistance is still an important clinical problem. Multiple potential resistance mechanisms to platinum-based chemotherapies and PARPi have been explored [7], but the exact mechanism is still undefined.

Human cell division cycle associated 8 (CDCA8), also known as Borealin or Dasar B, is an inseparable part of the vertebrate chromosomal passenger complex (CPC) [8, 9]. CPC consists of at least four proteins (AURKB, INCENP, BIRC5/survivin and CDCA8) [10-13] that play an important role in the regulation of the cell mitosis process and tumorigenesis [14-17]. CDCA8 has been shown to be highly expressed, to be related to poor prognosis and to participate in the tumorigenesis of bladder cancer [18], lung cancer [9], breast cancer [19, 20] and cutaneous melanoma [13]. CDCA8 had higher expression in chemoresistant papillary serous ovarian cancers than in chemosensitive cancers [21]. However, the exact role of CDCA8 in ovarian cancer remains unexplored.

In this study, we aimed to explore the biological functions of CDCA8 in ovarian cancer. Moreover, we evaluated the preclinical efficacy of silencing CDCA8 in combination with olaparib or cisplatin in ovarian cancer cells. Furthermore, the underlying mechanism was investigated in vitro. Finally, we attempted to elucidate the regulatory mechanism of CDCA8 in ovarian cancer.

Materials and methods

Patients and tissue samples

The high-grade serous ovarian cancer (HGSOC) tissue specimens for Western blot and real-time quantitative PCR (RT-qPCR) were from patients with primary ovarian serous carcinoma without previous surgery or chemotherapy, while the fallopian tube (FT) tissues were from patients who received hysterectomy and bilateral salpingo-oophorectomy due to benign gynecologic tumors. Ethical approval was obtained from the Ethics Committee of Shandong University. All patients provided written informed consent.

Cell lines and cell culture

A2780 (RRID: CVCL_0134) and HEY (RRID: CVCL_0297) cell lines were kind gifts from Jianjun Wei's Laboratory. HEK293T (RRID: CVCL_0063) cells were purchased from the Chinese Academy of Sciences (Shanghai, China). SKOV3 (RRID: CVCL_0532) cell lines were obtained from American Type Culture Collection (ATCC, Manassas, VA, USA). A2780 cells were cultured in RPMI 1640 supplemented with 10% fetal bovine serum (FBS); HEK293T, HEY and SKOV3 cells were maintained in Dulbecco's modified Eagle's medium (DMEM) supplemented with 10% FBS (all from Gibco, Grand Island, NY, USA). All cells were cultured in a humidified incubator at 37°C with 5% CO_2. All cell lines were identified within 3 years by short tandem repeat profiling and conformed to be mycoplasma free.

Antibodies and reagents

Antibodies against RAD51 (ab133534), γH2AX (ab26350) and MYBL2 (ab12296) were from Abcam (Cambridge, UK); antibody against CDCA8 (DF6115) was purchased from Affinity (Affinity Biosciences, China); antibody against BrdU-FITC (364104) was from Biolegend, and an antibody against β-actin (A5441) was purchased from Sigma-Aldrich (St. Louis, MO, USA); CDDP (PHR1624) was purchased from Sigma-Aldrich (St. Louis, MO, USA); Olaparib (AZD2281) and BrdU (S7918) were purchased from Selleck Chemicals (Houston, TX, USA).

Bioinformatics analysis

The GEO database was searched to download datasets contain gene expression of ovarian cancer and normal control (GSE14407), of resistance ovarian cancer cells and sensitive ones (GSE15709, GSE98559 and GSE58470). The Cancer Genome Atlas (TCGA), Oncomine (www.oncomine.org) and GEPIA (http://gepia.cancer-pku.cn/) databases were used to analyze the mRNA expression of serous ovarian cancer and normal tissues. The Cancer Cell Line Encyclopedia (CCLE, portals.broadinstitute.org) database was searched to download the expression profile of ovarian cancer cells, then the "limma" package of R software was employed to identify the co-expression genes of TOP2A and CDCA8 with the filter of "correlation > 0.5", "P < 0.001". Subsequently, the co-expression genes were analyzed with the clusterProfiler package of R software to performed the Kyoto Encyclopedia of Genes and Genomes (KEGG) analysis. The cBioPortal website (https://www.cbioportal.org) was used to visualize coexpressed genes with CDCA8. Cistrome (https://cistrome.org) and JASPAR (http://jaspar.binf.ku.dk) websites were used to search for potential transcription factors of CDCA8.

IHC

Immunohistochemical (IHC) staining was performed on 4 μm sections. Tissue sections were deparaffinized in xylene and a graded series of ethanol. After antigen retrieval, the slides were incubated with a primary antibody at 4°C overnight. The I-View 3,3'-diaminobenzidine (DAB; ZSGB-BIO, Beijing, China) detection system was used to detect the staining.

RNA isolation and RT-qPCR

Total RNA was extracted with TRIzol reagent (15596018, Invitrogen). cDNA was synthesized using the PrimeScript RT Reagent Kit (RR037A, TaKaRa, Kyoto, Japan). RT-qPCR was performed with SYBR Premix Ex Taq (RR420A, TaKaRa) on the 7900HT Fast Real-Time PCR System (Applied Biosystems, Waltham, MA, USA). The mRNA levels of specific genes were normalized against those of β-actin using the comparative Ct method ($2^{-\Delta\Delta Ct}$). The primers used are shown in the Table S1.

Protein extraction and western blotting

Cells were harvested and lysed in cell lysis buffer for Western blotting and IP (P0013, Beyotime, Shanghai, China) with PMSF (1%). The protein concentration was quantified with a BCA Protein Assay kit (Merck Millipore, USA). Proteins were separated by SDS-PAGE and transferred to PVDF membranes (Merck Millipore, Burlington, MA, USA) followed by blocking for 1-2 h with 5% skim milk and an incubation with primary antibodies at 4°C overnight. On the second day, the membranes were incubated with appropriate horseradish peroxidase-conjugated secondary antibodies and detected with an enhanced chemiluminescence detection kit (ECL ORT2655, PerkinElmer, Waltham, MA, USA). β-actin was used as an endogenous control. The relative protein level was analyzed using ImageJ 1.47 (US National Institutes of Health).

Plasmid construction, lentivirus production and siRNA transfection

CDCA8 shRNA primers were synthesized by GenePharma (Shanghai, China) and cloned into a PLKO vector. The CDCA8 over-expression plasmid was purchased from GeneChem (Shanghai, China), while the PCMV vector was used as a mock control. psPAX2, pMD2.G, PLKO/shCDCA8 or PCMV/CDCA8 were co-transfected into HEK293T cells to produce lentivirus. Ovarian cancer cells (A2780, SKOV3 and HEY) at appropriate confluence were transfected with lentivirus for 24 h before selection with 2 μg/ml puromycin (Merck Millipore, USA) for 7 days to acquire cells with stable expression.

Specific siRNA and negative control siRNA (NC) synthesized by GenePharma (Shanghai, China) were transfected into cells at appropriate confluence with Lipofectamine 2000 reagent according to the manufacturer's protocol (11668-019, Invitrogen).

The sequences of specific siRNA and short hair RNA (shRNA) were as follows: siCDCA8, 5'-CAGCAGAAGCUAUUCAGACTT-3', siMYBL2: 5'-CAGACAAUGCUGUGAAGAATT-3', siNC: 5'-UUCUCCGAACGUGUCACGUTT-3'; shCDCA8, 5'-AACAGCAGAAGCTATTCAGAC-3', shMYBL2: 5'-GCCCAAGAGCACACCTGTTAA-3'.

Cell proliferation assay

The 3-[4,5-dimethylthiazol-2-yl]-2,5-diphenyl tetrazolium bromide (MTT) assay was used to detect the cell proliferation ability. A total of 800-1000 cells per well were seeded in 96-well plates and cultured for 5 days. Before detecting the absorbance, 10 μg MTT (Sigma-Aldrich, USA, 0.5 mg/ml) was added to each well, 4 h incubation was continued and the supernatant was replaced by 100 μl DMSO (Sigma-Aldrich, USA). A Varioskan Flash microplate reader (Thermo Scientific) was used to detect the absorbance value at 490 nm.

Colony formation assay

A total of 800-1000 cells were seeded in each well of 6-well plates and cultured for 10-14 days. After fixing with methanol and staining with 0.5% crystal violet, colonies containing more than 50 cells were counted.

Transwell assays

Transwell assays were performed in transwell chambers (8-μm pores, BD Biosciences, USA) inserted in 24-well plates without or with Matrigel (BD Biosciences, USA). The upper chambers were coated with 200 μl serum-free medium containing 1×10^5-2×10^5 cells, while the lower compartment contained 700 μl culture medium supplemented with 20% FBS. After incubating at 37°C for an appropriate time, cells that had migrated to the lower surface of the membrane were fixed with methanol, stained in 0.5% crystal violet, observed and quantified under a light microscope.

Drug treatment

For survival assay, approximately 3×10^3 cells transfected with PLKO.NC or shCDCA8 were seeded in each well of 96-well plates and treated with indicated concentrations of olaparib or cisplatin. MTT assay was performed to detect cell viability.

For clonogenic assays, approximately 1.5×10^3 cells were seeded in each well of 6-well plates.

When the clones counted about 50 cells, indicated concentrations olaparib or cisplatin were added and incubated for 48 h.

Flow cytometry assay for cell cycle and apoptosis

Cells were harvested and stained with propidium iodide (PI) according to the manufacturer's protocol (CCS012, MultiSciences Biotech Co., Ltd.) to analyze the distribution of the cell cycle.

For BrdU incorporation, 10 μM BrdU was added 4 hours before harvesting. Cells were fixed with 75% EtOH overnight at -20°C, then treated with 2 N HCl/0.5% Triton X-100 and 0.1 M Na2-B4O7 (A610480, Sangon Biotech, Shanghai, China). Cells were stained with anti-BrdU-FITC (Biolegend, 364104) in the dark for 30 minutes followed by staining with PI for 5 minutes. Stained cells were detected by flow cytometry (FC500, Beckman Coulter, Brea, CA, USA) within one hour.

Apoptosis was quantified with annexin V-FITC and PI. Treated cells were harvested, rinsed twice with PBS and resuspended in 1 × binding buffer (556547, BD Bioscience, Franklin Lakes, NJ, USA). Before detection by flow cytometry, resuspended cells were stained with FITC Annexin V for 25 min and PI for 15 min in the dark at room temperature. The results were analyzed using FlowJo X 10.0.7 R2 software.

Immunofluorescence assay

Cells were fixed with 4% paraformaldehyde for 15 min, blocked with normal goat serum at room temperature (RT) for 30 min, and incubated with γH2AX (ab26350; Abcam; dilution 1:100) or RAD51 (ab133534; Abcam; dilution 1:100) antibodies overnight at 4°C. On the second day, cells were incubated with donkey anti-rabbit IgG Alexa Fluor-488 or goat anti-mouse IgG Alexa Fluor-594 (1:150; Invitrogen, Waltham, MA, USA) for 1 h at 37°C in the dark. The nuclei were counterstained with DAPI. Images were captured by Zeiss LSM 780 (Carl Zeiss, Jena, Germany).

Tumor formation assay in nude mice

HEY cells transfected with PLKO.NC and shCDCA8 were harvested, washed and resuspended in PBS. Next, 5×10^6 cells in 150 μl PBS were subcutaneously injected into the left armpit of each mouse. The tumor volumes were measured once every two days using the equation: length × width^2 × 0.5. Fourteen days post-injection, the mice were sacrificed and dissected, the tumors were photographed, weighed and the tumor volumes were calculated. Female athymic BALB/c nude mice (4-5 weeks old; NBRI of Nanjing University, Nanjing, China) were maintained in a pathogen-free facility. All animal experiments were performed with the approval of the Shandong University Animal Care and Use Committee.

Luciferase reporter assay

Cells were transiently cotransfected with PCMV or MYBL2, PGL4.26 vector or CDCA8 full-length promoter and pRL-TK using Lipofectamine 2000 for 48 h. Luciferase activity was measured using the Dual-Glo Luciferase Assay System (E2920, Promega, Fitchburg, WI, USA) following the manufacturer's instructions. The relative luciferase activity was determined by the ratio between firefly luminescence and renilla luminescence.

Chromatin immunoprecipitation (CHIP) assay

CHIP assay was carried out with Beyotime Chromatin immunoprecipitation kit (P2078, Beyotime, Shanghai, China) following the manufacturer's instructions. Briefly, HEY cells transfected with PCMV-MYBL2 were cross-linked in 1% formaldehyde solution for 10 min at room temperature. Then, 1.1 ml of glycine was added and incubated at room temperature for 5 min. The crosslinked samples were lysed in lysis buffer and sheared by sonification to obtain chromatin fragments that were 200-1000 bp. 10 μl supernatants were retained as input. The DNA-protein complexes were incubated overnight at 4°C with Flag antibody or negative control IgG. After immunoprecipitation, the chromatins were de-crosslinked at 65°C for 4 h and DNA was purified before conducting PCR. The sequences for CDCA8 promoter were as follows: CDCA8 forward, 5'-GGGGAGCGAGGAACGACA-3'; CDCA8 reverse, 5'-GGGTCTTCCGCCCAATGC-3'.

High-throughput differential gene expression analysis

The high-throughput mRNA-Seq experiments were conducted by Biomaker Technologies

(Beijing, China). Briefly, A2780 cells were transfected with siCDCA8 or NC (n = 3) for 48 h and total RNAs were extracted using TRIzol reagent. Sequencing libraries were generated using NEBNextR UltraTM Directional RNA Library Prep Kit for IlluminaR (NEB, USA) following manufacturer's recommendations, then the library preparations were sequenced on an Illumina Hiseq Xten platform and paired-end reads were generated. Subsequently, gene expression levels were estimated by fragments per kilobase of transcript per million fragments mapped (FPKM) and differential expression analysis of two groups was performed using the DESeq R package (1.10.1). Genes with an adjusted *P*-value < 0.05 and absolute value of log2 (Fold change) > 1 found by DESeq were assigned as differentially expressed genes (DEGs). Finally, gene function was annotated based on GO (Gene Ontology database) and KEGG (The database of Kyoto Encyclopedia of Genes and Genomes) databases. The Gene Ontology (GO) database can be used for functional enrichment analysis from cellular component (CC), molecular function (MF), and biological process (BP) respects. The GO enrichment analysis of the DEGs was implemented by the clusterProfiler R package and the KEGG pathway that are significantly enriched of the DEGs was analyzed by DAVID website (https://david.ncifcrf.gov/tools.jsp).

Statistical analysis

All experiments were repeated at least 3 times independently. The data are expressed as the means ± SEMs. Significance between two and more than two groups was performed using Student's t test and oneway ANOVA, respectively by SPSS v22.0 (SPSS, Inc., Chicago, IL, USA). Images were processed using GraphPad Prism 8.00 (GraphPad Software, La Jolla, CA, USA) and Adobe Photoshop CC 2019 (Adobe, San Jose, CA, USA). P < 0.05 was considered statistically significant (#P > 0.05, *P < 0.05, **P < 0.01, ***P < 0.001).

Results

CDCA8 is key gene high expressed and correlated to chemoresistance in ovarian cancer

In order to identify genes that play a role in progression and chemoresistance in ovarian cancer, we focused on higher expressed genes in ovarian cancer especially cisplatin resistance ovarian cancer. We searched the GEO database and restricted our results to genes with log2 (Fold change) > 1 in GSE14407 and log2 (Fold change) > 0.5 in GSE15709, respectively. Within these restrictions, we found 8 genes that were significantly higher expressed and related to cisplatin resistance in ovarian cancer (**Figure 1A**). We focused on the top2 genes TOP2A and CDCA8. To confirm our findings, we searched TCGA, GEPIA and Oncomine databases and found that TOP2A and CDCA8 were obviously more highly expressed in serous ovarian cancer samples than in peritoneum or ovarian surface epithelial tissues (**Figure 1B-H**). Then we verified the expression of these two genes in cisplatin resistance ovarian cancer cells, as shown in **Figure 1I-N**, CDCA8 was higher expressed in cisplatin resistance A2780, SKOV3 and IGROV1 ovarian cancer cells compared with the sensitive ones, however, the expression of TOP2A was only higher in A2780 cells. We also found that the expression level of these two genes were higher in other cancers such as bladder, lung and breast cancer (**Figure 1O**, **1P**). Furthermore, the mRNA expression data of TOP2A and CDCA8 in ovarian cancer cells were also downloaded from the CCLE and KEGG pathway analysis was performed based on the co-expression genes of TOP2A and CDCA8, respectively. As shown in **Figure 1Q** and **1R**, they both participated in the cell cycle, DNA replication, oocyte meiosis and progesterone-mediated oocyte maturation, while CDCA8 also played a role in base excision repair, nucleotide excision repair and mismatch repair pathways which are important in the DNA damage repair, so we focused on CDCA8. Additionally, the mRNA and protein levels of CDCA8 in HGSOC and FT samples from patients were detected by RT-qPCR and Western blot, and the results showed that CDCA8 had significantly higher expression in HGSOC than in FT tissues (**Figures 1S**, **1T**, S2A). Immunohistochemistry (IHC) was performed to assess the expression profile of CDCA8 in HGSOC. CDCA8-positive staining was located in both the nucleus and cytoplasm, and CDCA8 expression in HGSOC tissues was significantly higher than that in FT tissues (**Figure 1U**). These results suggest that CDCA8 was distinctively overexpressed in ovarian cancer especially in cisplatin resistance ones, implying a potent role of CDCA8 in the progression and chemoresistance of ovarian cancer.

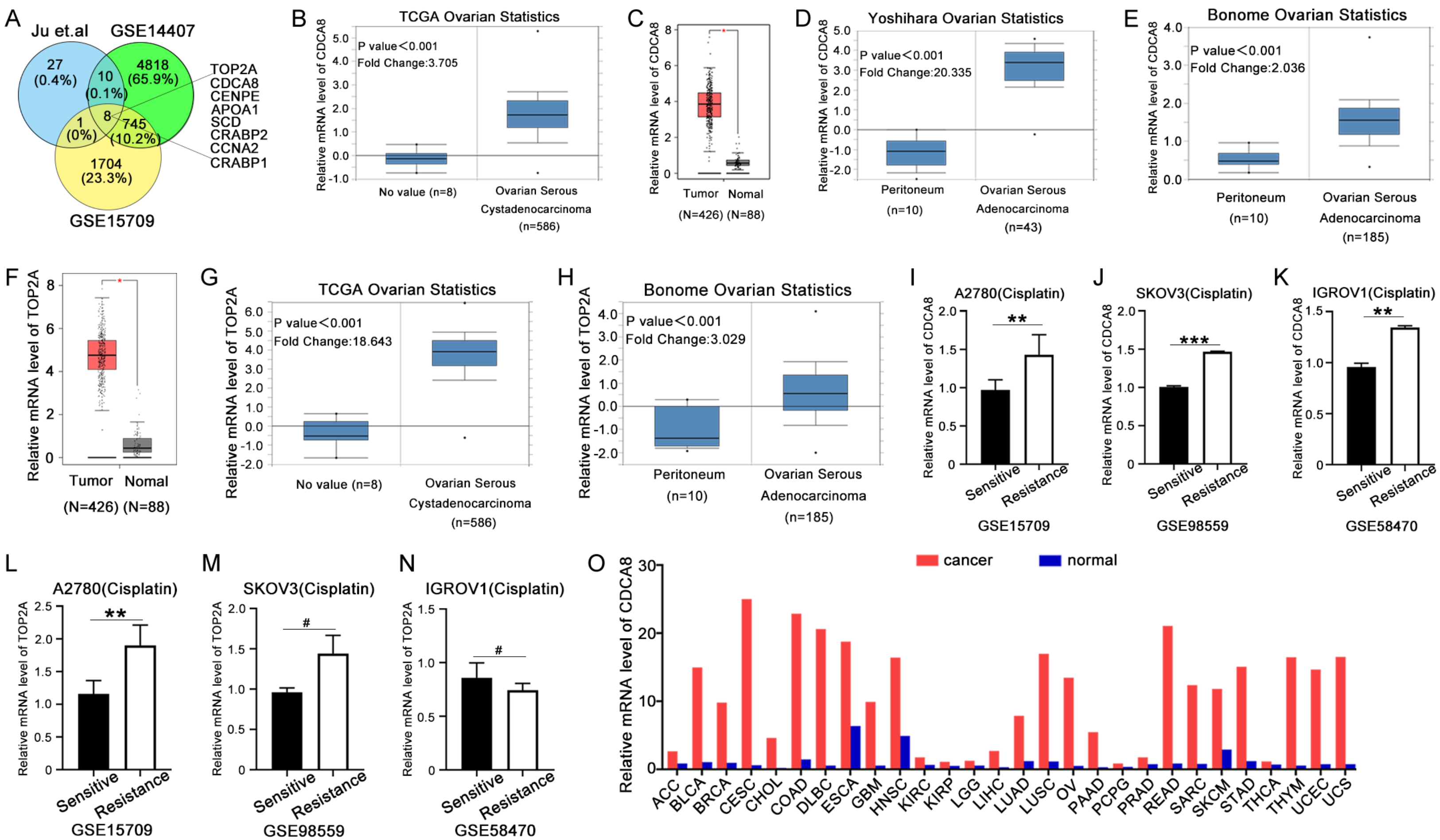
A
Ju et.al
GSE14407
GSE15709
27 (0.4%)
4818 (65.9%)
10 (0.1%)
8
1 (0%)
745 (10.2%)
1704 (23.3%)
TOP2A
CDCA8
CENPE
APOA1
SCD
CRABP2
CCNA2
CRABP1
B
TCGA Ovarian Statistics
P value<0.001
Fold Change:3.705
Relative mRNA level of CDCA8
No value (n=8)
Ovarian Serous Cystadenocarcinoma (n=586)
C
Relative mRNA level of CDCA8
Tumor
Nomal
(N=426) (N=88)
D
Yoshihara Ovarian Statistics
P value<0.001
Fold Change:20.335
Relative mRNA level of CDCA8
Peritoneum (n=10)
Ovarian Serous Adenocarcinoma (n=43)
E
Bonome Ovarian Statistics
P value<0.001
Fold Change:2.036
Relative mRNA level of CDCA8
Peritoneum (n=10)
Ovarian Serous Adenocarcinoma (n=185)
F
Relative mRNA level of TOP2A
Tumor
Nomal
(N=426) (N=88)
G
TCGA Ovarian Statistics
P value<0.001
Fold Change:18.643
Relative mRNA level of TOP2A
No value (n=8)
Ovarian Serous Cystadenocarcinoma (n=586)
H
Bonome Ovarian Statistics
P value<0.001
Fold Change:3.029
Relative mRNA level of TOP2A
Peritoneum (n=10)
Ovarian Serous Adenocarcinoma (n=185)
I
A2780(Cisplatin)
Relative mRNA level of CDCA8
Sensitive
Resistance
GSE15709
J
SKOV3(Cisplatin)
Relative mRNA level of CDCA8
Sensitive
Resistance
GSE98559
K
IGROV1(Cisplatin)
Relative mRNA level of CDCA8
Sensitive
Resistance
GSE58470
L
A2780(Cisplatin)
Relative mRNA level of TOP2A
Sensitive
Resistance
GSE15709
M
SKOV3(Cisplatin)
Relative mRNA level of TOP2A
Sensitive
Resistance
GSE98559
N
IGROV1(Cisplatin)
Relative mRNA level of TOP2A
Sensitive
Resistance
GSE58470
O
cancer
normal
Relative mRNA level of CDCA8
ACC BLCA BRCA CESC CHOL COAD DLBC ESCA GBM HNSC KIRC KIRP LGG LIHC LUAD LUSC OV PAAD PCPG PRAD READ SARC SKCM STAD THCA THYM UCEC UCS

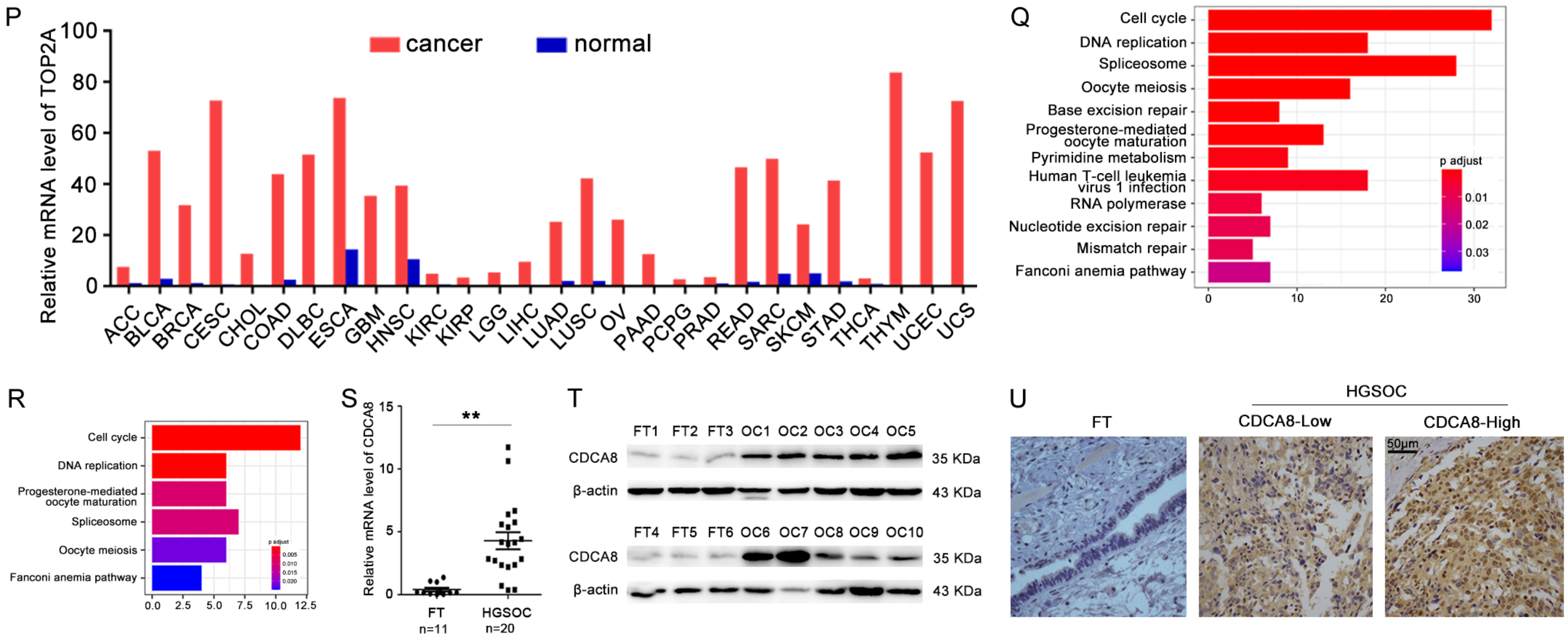

Figure 1. CDCA8 is key gene high expressed and correlated to chemoresistance in ovarian cancer. (A) Public data sets were used to identify genes associated with chemoresistance of ovarian cancer. (B-H) Oncomine and GEPIA databases showed the mRNA expression of CDCA8 and TOP2A in serous ovarian carcinoma and normal controls. (I-N) The mRNA expression level of CDCA8 and TOP2A in cisplatin resistance A2780, SKOV3 and TGROV1 cells. (O and P) The mRNA level of CDCA8 and TOP2A in pan cancer. (Q and R) Pathway analysis showed the signal pathways participated in by co-expression genes of CDCA8 and TOP2A. (S and T) The mRNA and protein levels of CDCA8 in HGSOC and FT tissues. (U) Representative IHC staining of CDCA8 in HGSOC and FT tissues (200 ×), Scale bar: 50 μm. (Data are mean ± SEM, $^{\#}P > 0.05$, $^{*}P < 0.05$, $^{**}P < 0.01$, $^{***}P < 0.001$, n = 3).

CDCA8 promotes the proliferation and motility of ovarian cancer

To explore the potent role of CDCA8 in the development and progression of ovarian cancer, A2780, SKOV3 and HEY cells were stably transfected with shCDCA8 to knockdown CDCA8 expression (**Figures 2A**, S2B). Compared to the control, upon CDCA8 silencing, fewer viable cells were observed during cultivation of these three ovarian cancer cells (**Figure 2B**). Colony formation assays also showed that growth was retarded in the shCDCA8 groups (**Figure 2C**). To investigate whether CDCA8 could influence the migration and invasion abilities of ovarian cancer cells, we performed transwell assays. The results showed that CDCA8 silencing dramatically decreased cell migration and invasion to the lower surface of the membrane (**Figure 2D**, **2E**). To further explore the effects of CDCA8 on the tumorigenesis of ovarian cancer in vivo, HEY cells transfected with PLKO.NC or shCDCA8 were subcutaneously injected into the left armpit of female nude mice. The results showed that the volumes of the tumors in the shCDCA8 group were evidently decreased compared with those in the control group (**Figure 2F**, **2G**). The expression level of CDCA8 in tumor samples was detected again by IHC. As shown in **Figure 2H**, the CDCA8 expression level was obviously decreased in the shCDCA8 group. Additionally, the number of Ki-67 positive cells was distinctively decreased in the shCDCA8 group (**Figure 2H**). To confirm the promotive role of CDCA8 in ovarian cancer, CDCA8-overexpressing lentiviruses (CDCA8) were transfected to SKOV3 and HEY cells to overexpress CDCA8 (**Figures 2I**, S2C). Conversely, overexpression of CDCA8 obviously accelerated the proliferation and colony formation of SKOV3 and HEY cells (**Figure 2J**, **2K**). The migration and invasion of ovarian cancer cells with CDCA8 overexpression were significantly promoted (**Figure 2L**). These findings suggest that CDCA8 promoted proliferation, migration and invasion of ovarian cancer.

CDCA8 knockdown renders ovarian cancer cells more sensitive to olaparib and cisplatin

A2780 and SKOV3 cells were treated with olaparib for 48 h and 72 h respectively, then MTT assay was performed to show the cell survival rate and IC_{50} (the drug concentration that inhibited cell viability by 50%) of these cells. As shown in **Figures 3A** and S1, the cell viability decreased in a dose-dependent manner and the IC_{50} values of olaparib for A2780 and SKOV3 cells were 25.92 and 67.76 μM, respectively. To confirm the role of CDCA8 in the sensitivity of ovarian cancer cells to olaparib, A2780 and SKOV3 cells were treated with 25 μM and 100 μM olaparib for 48 h, separately. Western blot assays demonstrated that the CDCA8 level increased after olaparib treatment (**Figures 3B**, S2D). Cells were treated with the indicated concentrations of olaparib after stable transfection with PLKO.NC or shCDCA8, and MTT assays were performed to measure cell viability 48 h after drug treatment. We observed that the IC_{50} was lower in the shCDCA8 group than in the control group (**Figure 3C**). The colony formation assays also indicated that ovarian cancer cells with CDCA8 knockdown were more sensitive to olaparib than control cells (**Figure 3D**). Due to the similar drug mechanism between olaparib and cisplatin, we also detected the effect of CDCA8 knockdown on the sensitivity to cisplatin. As shown in **Figures 3E-G** and S2E, cisplatin treatment elevated the expression of CDCA8, and CDCA8 inhibition significantly enhanced the ovarian cancer cells response to cisplatin.

Next-generation sequencing (NGS) assay reveals signaling pathways involved in the function of CDCA8

To identify the underlying mechanisms involved in CDCA8-induced biological functions and insensitivity to chemotherapy, Next-generation sequencing (NGS) was performed in CDCA8-knockdown (siCDCA8) and negative control (NC) A2780 cells. Differentially expressed genes (DEGs) were selected according to their fold change (> 2-fold) and statistical significance ($P < 0.05$). A total of 1263 genes were found, including 760 upregulated and 503 downregulated genes (**Figure 4A**; Table S2). Biological process (BP) analysis revealed that DEGs mainly participated in the positive regulation of cell proliferation, negative regulation of apoptosis, cell division, negative regulation of cell differentiation, sister chromatid cohesion, DNA damage response and DNA replication initiation (**Figure 4B**). Kyoto Encyclopedia of Genes and Genomes (KEGG) analysis was performed to explore the main signaling pathways in which the DEGs participated. The results showed that the downregulated genes mainly participated in the cell cycle, DNA replication,

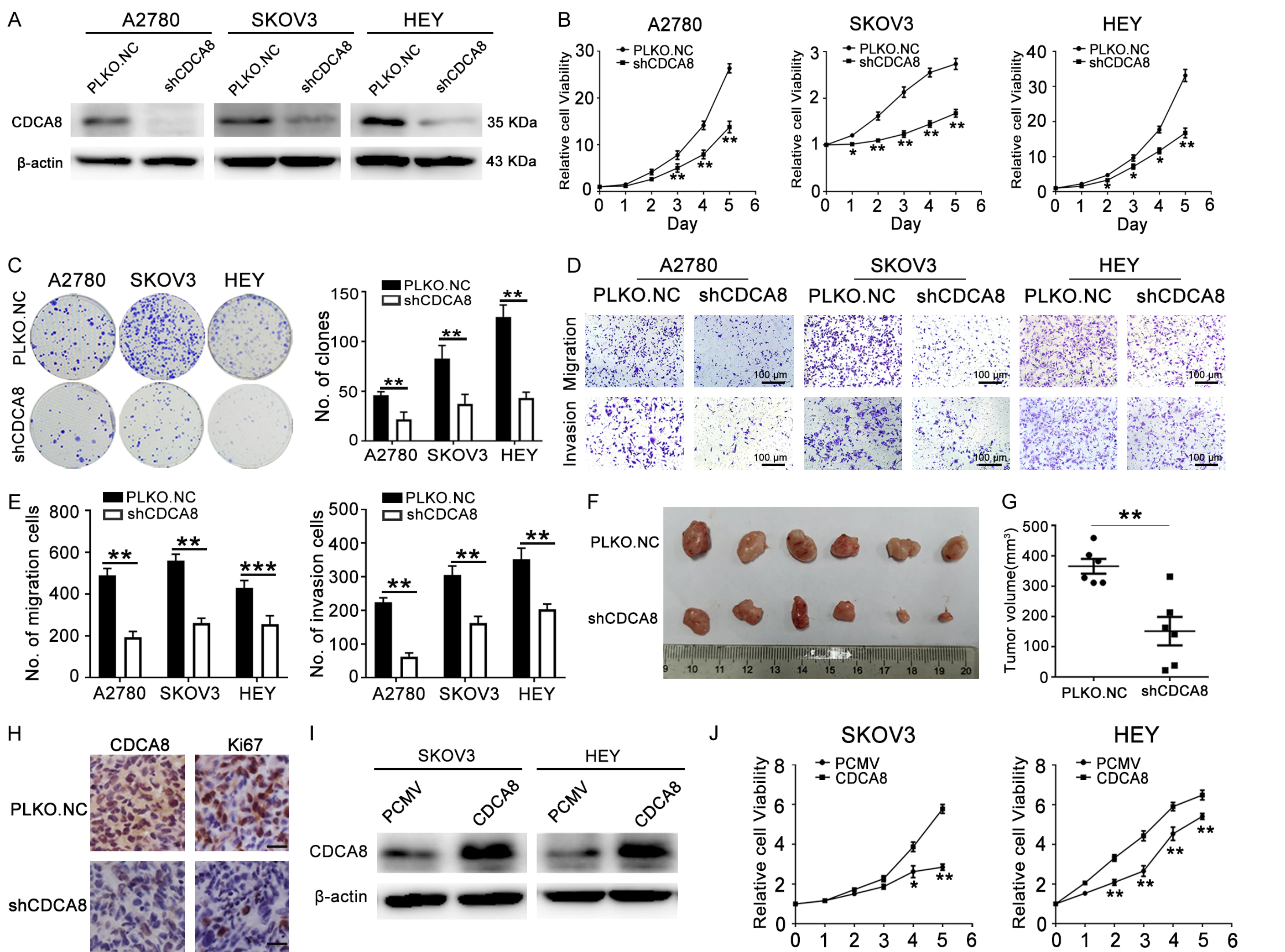
A
A2780
SKOV3
HEY
PLKO.NC
shCDCA8
CDCA8
β-actin
35 KDa
43 KDa
B
Relative cell Viability
Day
C
No. of clones
D
Migration
Invasion
100 μm
E
No. of migration cells
No. of invasion cells
F
G
Tumor volume(mm³)
H
Ki67
I
PCMV
J

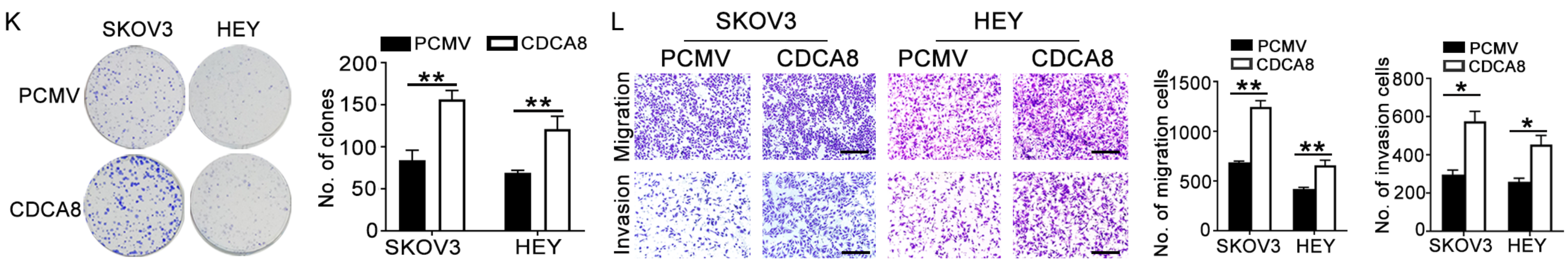

Figure 2. CDCA8 promotes the proliferation and motility of ovarian cancer. (A) The protein level of CDCA8 in ovarian cancer cells after transfection with PLKO.NC or shCDCA8. (B) Proliferative curve showed the effect of knocking down CDCA8 on A2780, SKOV3 and HEY cells. (C) The effect of CDCA8 inhibition on colony formation. (D) Transwell assays showed the effects of CDCA8 knockdown on migration and invasion of A2780, SKOV3 and HEY cells (200 ×), Scale bar: 100 μm. (E) Quantification of the number of migration and invasion cells in (D). (F) Tumors photographs were shown. (G) Tumors volumes of each group. (H) Representative IHC staining of Ki-67 and CDCA8 in tumor tissues (400 ×), Scale bar: 25 μm. (I) The protein level of CDCA8 in SKOV3 and HEY cells after transfection with PCMV or CDCA8. (J) MTT assay showed the effect of CDCA8 on SKOV3 and HEY cells. (K) Effect of CDCA8 overexpression on the colony formation of SKOV3 and HEY cells. (L) In SKOV3 and HEY cells, over-expression of CDCA8 affected the migration and invasion ability (200 ×), Scale bar: 100 μm. (Data are mean ± SEM, **P* < 0.05, ***P* < 0.01, ****P* < 0.001, n = 3; for mouse, n = 6).

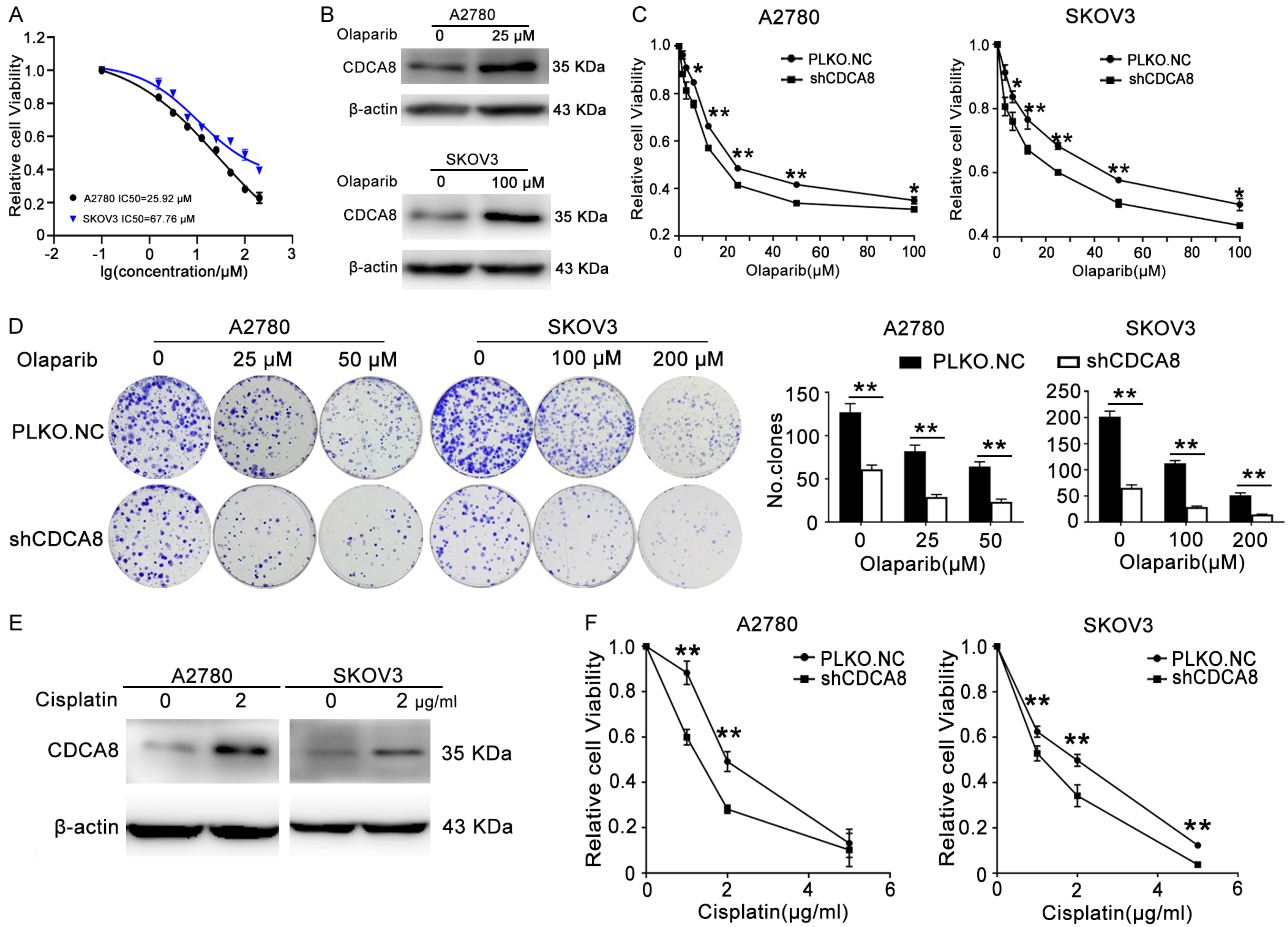
A
Relative cell Viability
A2780 IC50=25.92 μM
SKOV3 IC50=67.76 μM
lg(concentration/μM)
B
A2780
Olaparib 0 25 μM
CDCA8 35 KDa
β-actin 43 KDa
SKOV3
Olaparib 0 100 μM
CDCA8 35 KDa
β-actin 43 KDa
C
A2780
SKOV3
PLKO.NC
shCDCA8
Relative cell Viability
Olaparib(μM)
D
A2780
SKOV3
Olaparib 0 25 μM 50 μM 0 100 μM 200 μM
PLKO.NC
shCDCA8
No.clones
Olaparib(μM)
E
A2780
SKOV3
Cisplatin 0 2 0 2 μg/ml
CDCA8 35 KDa
β-actin 43 KDa
F
A2780
SKOV3
PLKO.NC
shCDCA8
Relative cell Viability
Cisplatin(μg/ml)

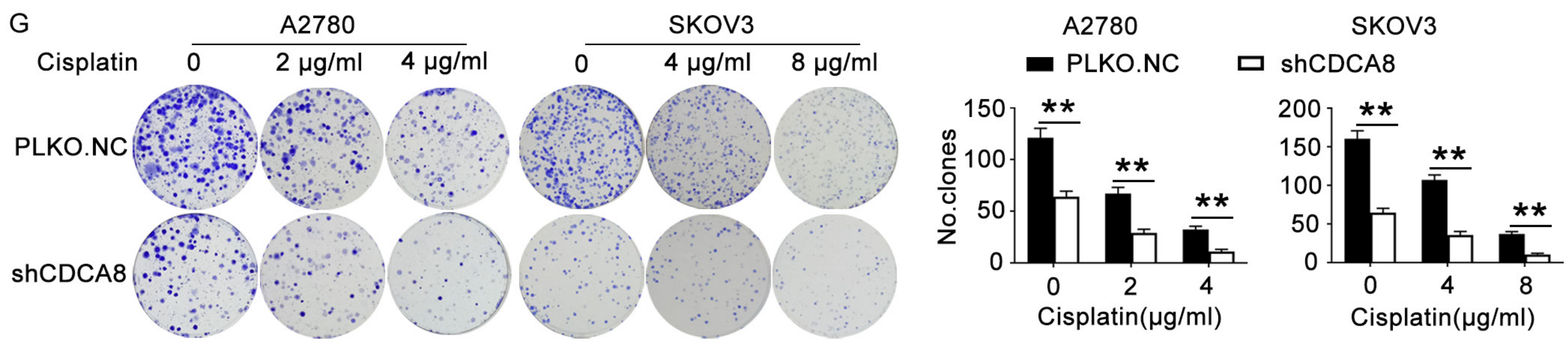

Figure 3. CDCA8 knockdown renders ovarian cancer cells sensitive to olaparib and cisplatin. (A) The IC_{50} of olaparib in A2780 and SKOV3 cells. (B) A2780 and SKOV3 cells were treated with 25 μM and 100 μM olaparib for 48 h, respectively. The expression of CDCA8 protein level was analyzed by western blot. (C and D) A2780 and SKOV3 cells transfected with PLKO.NC or shCDCA8 were treated with olaparib for 48 h at indicated concentrations. MTT assays (C) and colony formation assays (D) were performed to detect cell viability and colony forming capacity. (E) A2780 and SKOV3 cells were treated with 2 μg/ml cisplatin for 48 h. The protein expression level of CDCA8 was analyzed by Western blot. (F and G) A2780 and SKOV3 cells transfected with PLKO.NC or shCDCA8 were treated with cisplatin for 48 h at indicated concentrations. MTT assays (F) and colony formation assays (G) were performed to detect cell viability and colony forming capacity. (Data are mean ± SEM, **P* < 0.05, ***P* < 0.01, n = 3).

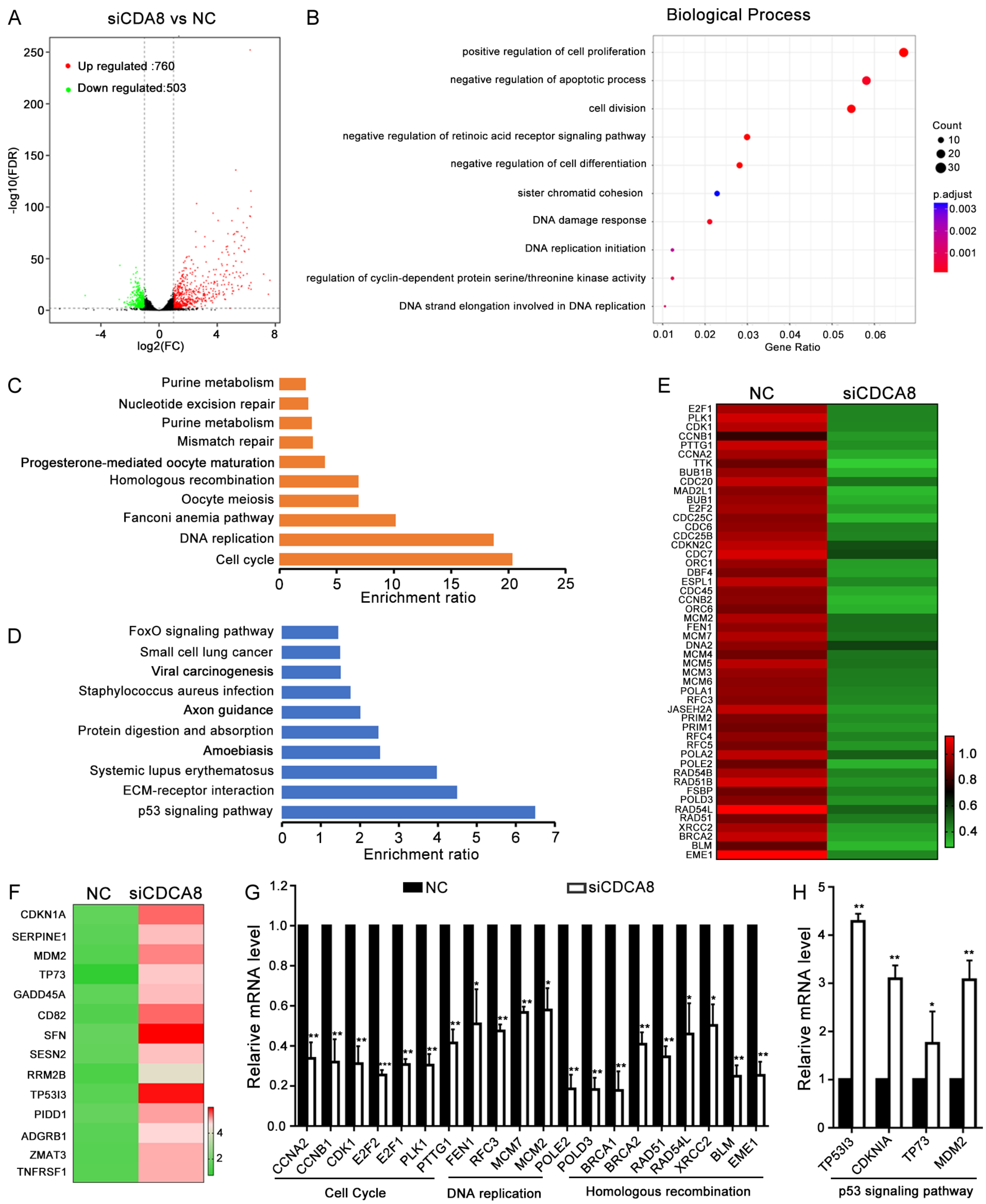

Figure 4. NGS analysis of CDCA8 affected signal pathways. A2780 cells were transfected with siCDCA8 or NC for 48 h and NGS was performed to determine the mRNA expression profile. (A) DEGs between siCDCA8 and NC groups were exhibited in Volcano plot. (B) Biological Process analysis showed the main process participated in by DEGs. (C) The downregulated pathways participated in by the DEGs. (D) The upregulated pathways participated in by the DEGs. (E and F) Heatmap of DEGs in the cell cycle, DNA replication, homologous recombination and P53 signaling pathway between siCDCA8 and NC groups. (G and H) Representative DEGs between siCDCA8 and NC groups were verified by RT-qPCR in A2780 cells. (Data are mean ± SEM, **P* < 0.05, ***P* < 0.01, ****P* < 0.001, n = 3).

Fanconi anemia pathway, Oocyte meiosis and homologous recombination (**Figure 4C**). While the top upregulated pathway was the p53 signaling pathway (**Figure 4D**). We showed partial

DEGs and performed RT-qPCR to verify the changes in the representative DEGs involved in the cell cycle, DNA replication, homologous recombination and the p53 signaling pathway (**Figure 4E-H**). We speculated that CDCA8 mediated the sensitivity of ovarian cancer cells to olaparib and cisplatin through the cell cycle, DNA replication and homologous recombination pathways which were related to the mechanism of these drugs.

Knockdown of CDCA8 sensitizes ovarian cancer to olaparib and cisplatin by regulating cell cycle, apoptosis and homologous recombination-mediated repair

SKOV3 and HEY cells transfected with PLKO.NC or shCDCA8 were incubated with DMSO or olaparib for 48 h at appropriate concentration. Cell cycle and BrdU incorporation analysis of olaparib-treated cancer cells revealed that combination treatment with knocking down CDCA8 significantly increased the number of cells in G2/M phase (**Figure 5A**, **5B**). We also performed an apoptosis assay to demonstrate whether CDCA8 knockdown affects olaparib sensitivity by increasing the proportion of cells undergoing apoptosis. As shown in **Figure 5C**, there were more apoptotic cells in the shCDCA8 group than in the control group, and olaparib treatment increased the proportion of apoptotic cells more obviously in the shCDCA8 group. To explore whether depletion of CDCA8 sensitize ovarian cancer cells to olaparib by inducing DNA damage and reducing HR-mediated repair, immunofluorescence analysis was performed, and the number of γH2AX and RAD51 foci inside the cells was counted. CDCA8 knockdown or olaparib monotherapy groups had increased γH2AX expression and reduced RAD51 expression, while these changes were more obvious in the group treated with the combination of CDCA8 silencing and olaparib (**Figure 5D**, **5E**).

CDCA8 is transcriptionally regulated by MYBL2

To determine the regulatory mechanism of CDCA8 in ovarian cancer, we searched the Cistrome and JASPAR online databases for potential transcription factors that targeted the CDCA8 promoter. Finally, we focused on MYBL2. To determine the direct regulatory role of MYBL2 and CDCA8, we first detected the mRNA and protein levels of CDCA8 after knockdown or overexpression of MYBL2. The results showed that CDCA8 expression decreased with silencing of MYBL2 and that overexpression of MYBL2 increased the CDCA8 level (**Figures 6A**, **6B**, S2F). Then, we performed RT-qPCR to assess the expression profile of MYBL2 in ovarian cancer tissues and FT samples. As shown in **Figure 6C**, MYBL2 was significantly overexpressed in ovarian cancer tissues. Public databases were also searched to determine the differential expression of MYBL2 between ovarian cancer tissues and normal control tissues. MYBL2 was significantly more highly expressed in ovarian cancer samples than in peritoneum or ovarian surface epithelial tissues (**Figure 6D-G**). Moreover, a positive correlation between MYBL2 and CDCA8 was confirmed by online databases and RT-qPCR (**Figure 6H**, **6I**). Furthermore, we cloned the promotor of CDCA8 into the pGL4.26 vector to construct the CDCA8 promoter plasmid, and the pGL4.26 vector or CDCA8 promoter was then cotransfected into HEK293T, SKOV3 and HEY cells with PCMV or MYBL2 plasmids, separately. The results showed that MYBL2 overexpression increased the luciferase activity in cells transfected with the CDCA8 promoter (**Figure 6J**). Finally, ChIP-PCR was performed in HEY cells to confirm that MYBL2 could bind directly to the promoter of CDCA8 at the predicted potentially binding motif (CAGTCAA) about 424 bp upstream of the CDCA8 transcription start site (TSS) (**Figure 6K**, **6L**). Thus, MYBL2 could regulate CDCA8 expression through directly binding to the CDCA8 promoter in ovarian cancer cells.

MYBL2 acts as an oncogene in ovarian cancer

To further reveal the definite role of MYBL2 in ovarian cancer, MYBL2 was knocked down by shRNA (shMYBL2). MTT and colony formation assays were performed to assess the growth ability of ovarian cancer cells. After transfection with shMYBL2, the growth rate and colony formation ability of these cells decreased markedly compared to those of cells transfected with PLKO.NC (**Figure 7A**, **7B**). In the transwell assays, migration and invasion of A2780, SKOV3 and HEY cells transfected with shMYBL2 were evidently decreased compared to those of the control cells (**Figure 7C**, **7D**). These findings indicated that inhibition of MYBL2 impaired the growth and metastasis of ovarian cancer cells.

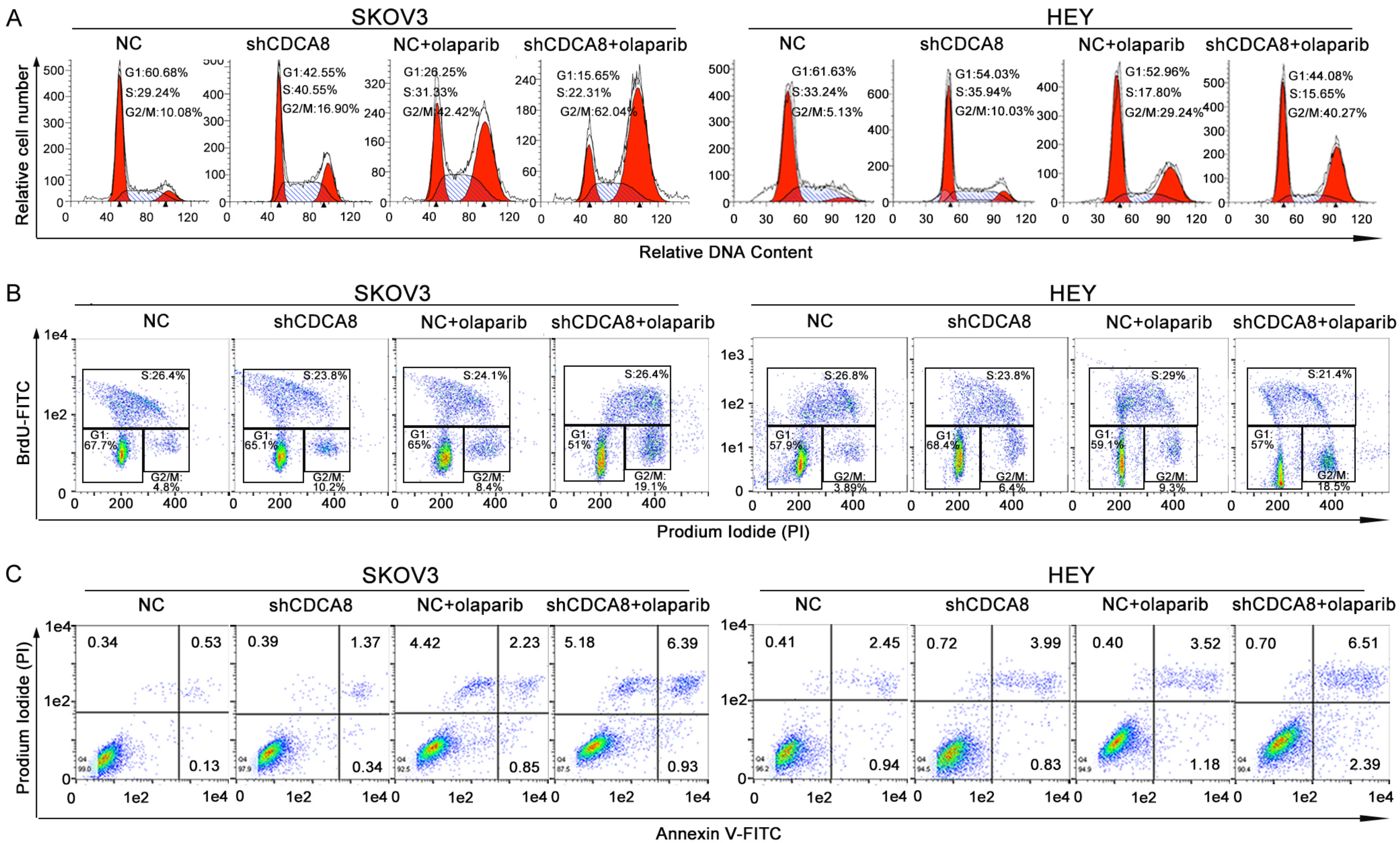
A
SKOV3
HEY
NC
shCDCA8
NC+olaparib
shCDCA8+olaparib
Relative cell number
G1:60.68%
S:29.24%
G2/M:10.08%
G1:42.55%
S:40.55%
G2/M:16.90%
G1:26.25%
S:31.33%
G2/M:42.42%
G1:15.65%
S:22.31%
G2/M:62.04%
G1:61.63%
S:33.24%
G2/M:5.13%
G1:54.03%
S:35.94%
G2/M:10.03%
G1:52.96%
S:17.80%
G2/M:29.24%
G1:44.08%
S:15.65%
G2/M:40.27%
Relative DNA Content
B
SKOV3
HEY
NC
shCDCA8
NC+olaparib
shCDCA8+olaparib
BrdU-FITC
S:26.4%
G1: 67.7%
G2/M: 4.8%
S:23.8%
G1: 65.1%
G2/M: 10.2%
S:24.1%
G1: 65%
G2/M: 8.4%
S:26.4%
G1: 51%
G2/M: 19.1%
S:26.8%
G1: 57.9%
G2/M: 3.89%
S:23.8%
G1: 68.4%
G2/M: 6.4%
S:29%
G1: 59.1%
G2/M: 9.3%
S:21.4%
G1: 57%
G2/M: 18.5%
Prodium Iodide (PI)
C
SKOV3
HEY
NC
shCDCA8
NC+olaparib
shCDCA8+olaparib
Prodium Iodide (PI)
0.34
0.53
0.13
0.39
1.37
0.34
4.42
2.23
0.85
5.18
6.39
0.93
0.41
2.45
0.94
0.72
3.99
0.83
0.40
3.52
1.18
0.70
6.51
2.39
Annexin V-FITC

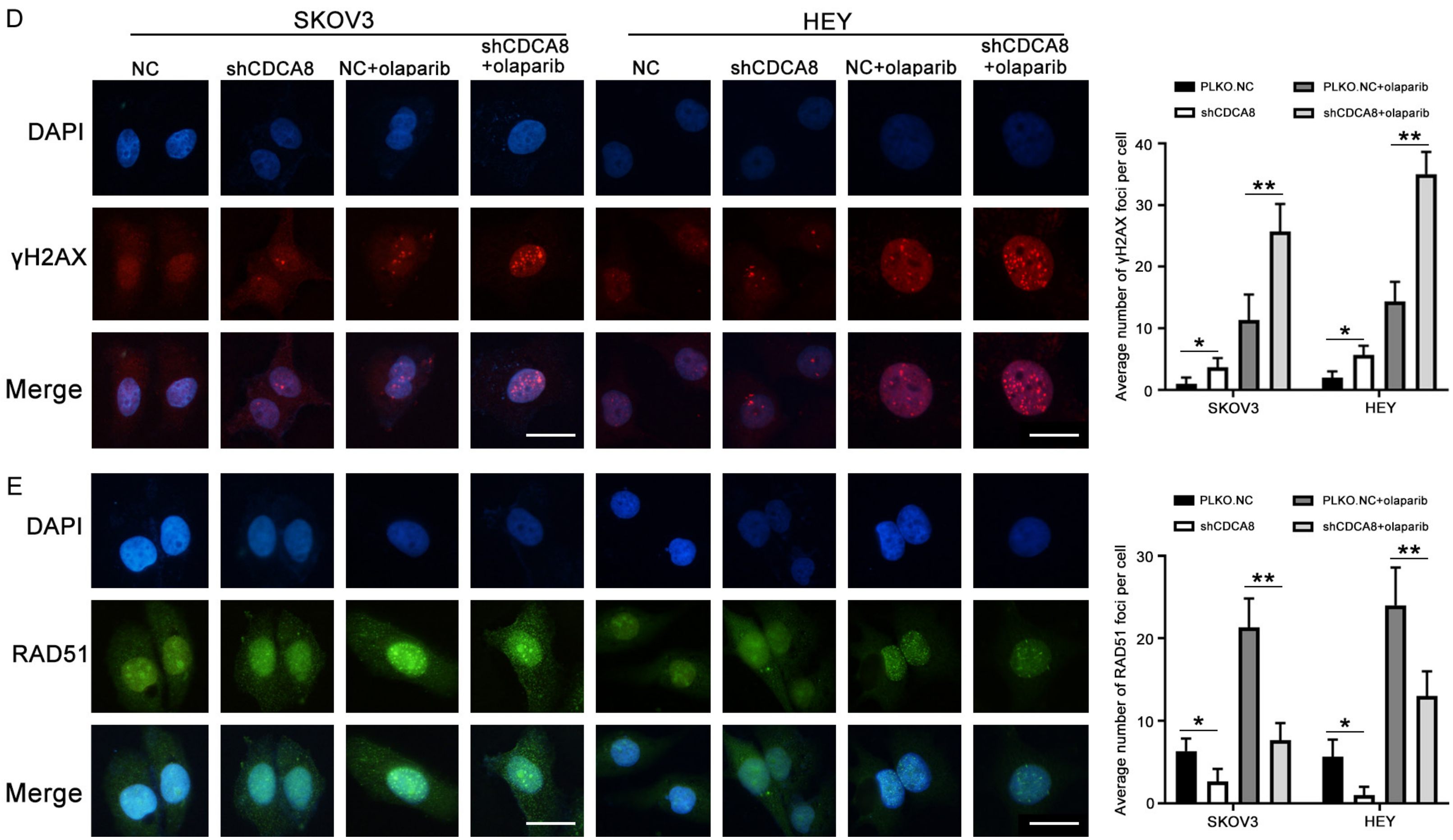

Figure 5. Knockdown CDCA8 increases olaparib sensitivity in SKOV3 and HEY cells by regulating the cell cycle, apoptosis and homologous recombination-mediated repair. HEY and SKOV3 cells transfected with PLKO.NC or shCDCA8 were treated with 40 μM and 100 μM olaparib for 48 h in cell cycle, apoptosis and immunofluorescence assays; for BrdU incorporation the concentration of olaparib was 3 μM and 5 μM, respectively. (A) Cell cycle analysis was performed by flow cytometry. (B) Cell cycle was analyzed via flow cytometry using BrdU incorporation. (C) Flow cytometry assays were performed to analyze the apoptosis. (D and E) The number of γH2AX and RAD51 foci were examined by immunofluorescence (400 ×). Scale bar: 10 μm. (Data are mean ± SEM, **P* < 0.05, ***P* < 0.01, n = 3).

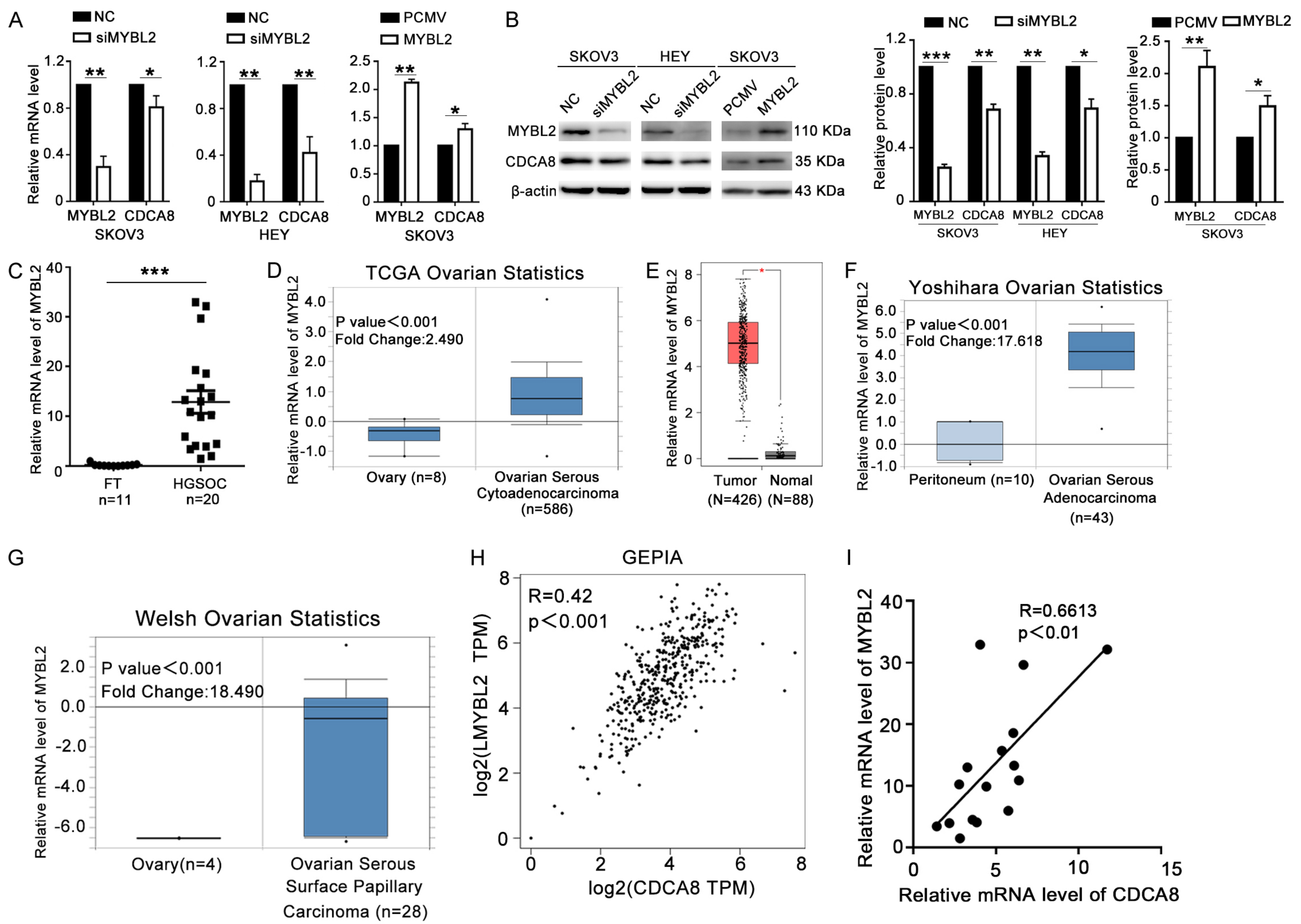

A
NC
siMYBL2
PCMV
MYBL2
Relative mRNA level
MYBL2 CDCA8
SKOV3
HEY
B
SKOV3 HEY SKOV3
NC siMYBL2 NC siMYBL2 PCMV MYBL2
MYBL2 110 KDa
CDCA8 35 KDa
β-actin 43 KDa
Relative protein level
C
Relative mRNA level of MYBL2
FT n=11
HGSOC n=20
D
TCGA Ovarian Statistics
P value<0.001
Fold Change:2.490
Ovary (n=8)
Ovarian Serous Cytoadenocarcinoma (n=586)
E
Tumor (N=426)
Nomal (N=88)
F
Yoshihara Ovarian Statistics
P value<0.001
Fold Change:17.618
Peritoneum (n=10)
Ovarian Serous Adenocarcinoma (n=43)
G
Welsh Ovarian Statistics
P value<0.001
Fold Change:18.490
Ovary(n=4)
Ovarian Serous Surface Papillary Carcinoma (n=28)
H
GEPIA
R=0.42
p<0.001
log2(LMYBL2 TPM)
log2(CDCA8 TPM)
I
R=0.6613
p<0.01
Relative mRNA level of MYBL2
Relative mRNA level of CDCA8

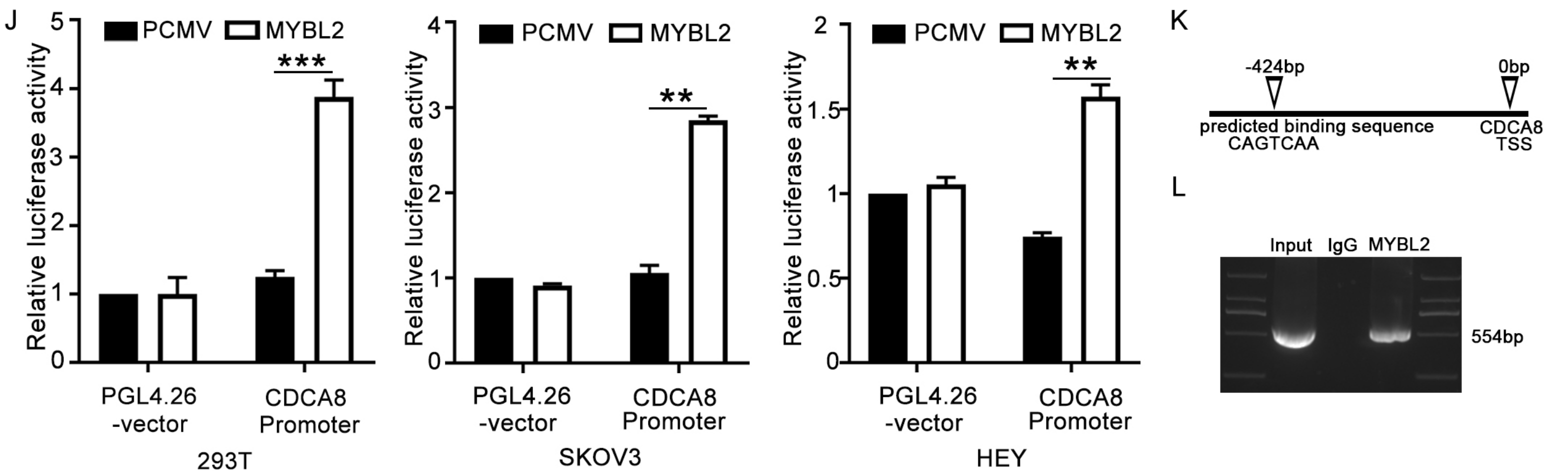

Figure 6. CDCA8 is transcriptionally regulated by MYBL2. (A and B) SKOV3 and HEY cells were transfected with NC, siMYBL2, PCMV or MYBL2 for 48 h. The mRNA and protein levels of CDCA8 and MYBL2 were determined by RT-qPCR (A) and western blot (B). (C) The mRNA level of MYBL2 in HGSOC tissues and FT tissues. (D-G) The expression of MYBL2 in ovarian carcinoma and normal controls in Oncomine and GEPIA datasets. (H and I) Correlation between expression levels of MYBL2 and CDCA8 from GEPIA database and in HGSOC tissues. (J) PCMV or MYBL2 plasmids were co-transfected into HEK293T, SKOV3 and HEY cells with CDCA8 promoter or pGL4.26 vector for 48 h and luciferase activity were measured. (K) Schematic illustration of the potential MYBL2-binding sites and sequence on CDCA8 promoter predicted by JASPAR. (L) ChIP-PCR assays were performed to identify that MYBL2 binds directly to CDCA8 promoter. (Data are mean ± SEM, *$P < 0.05$, **$P < 0.01$, ***$P < 0.001$, n = 3).

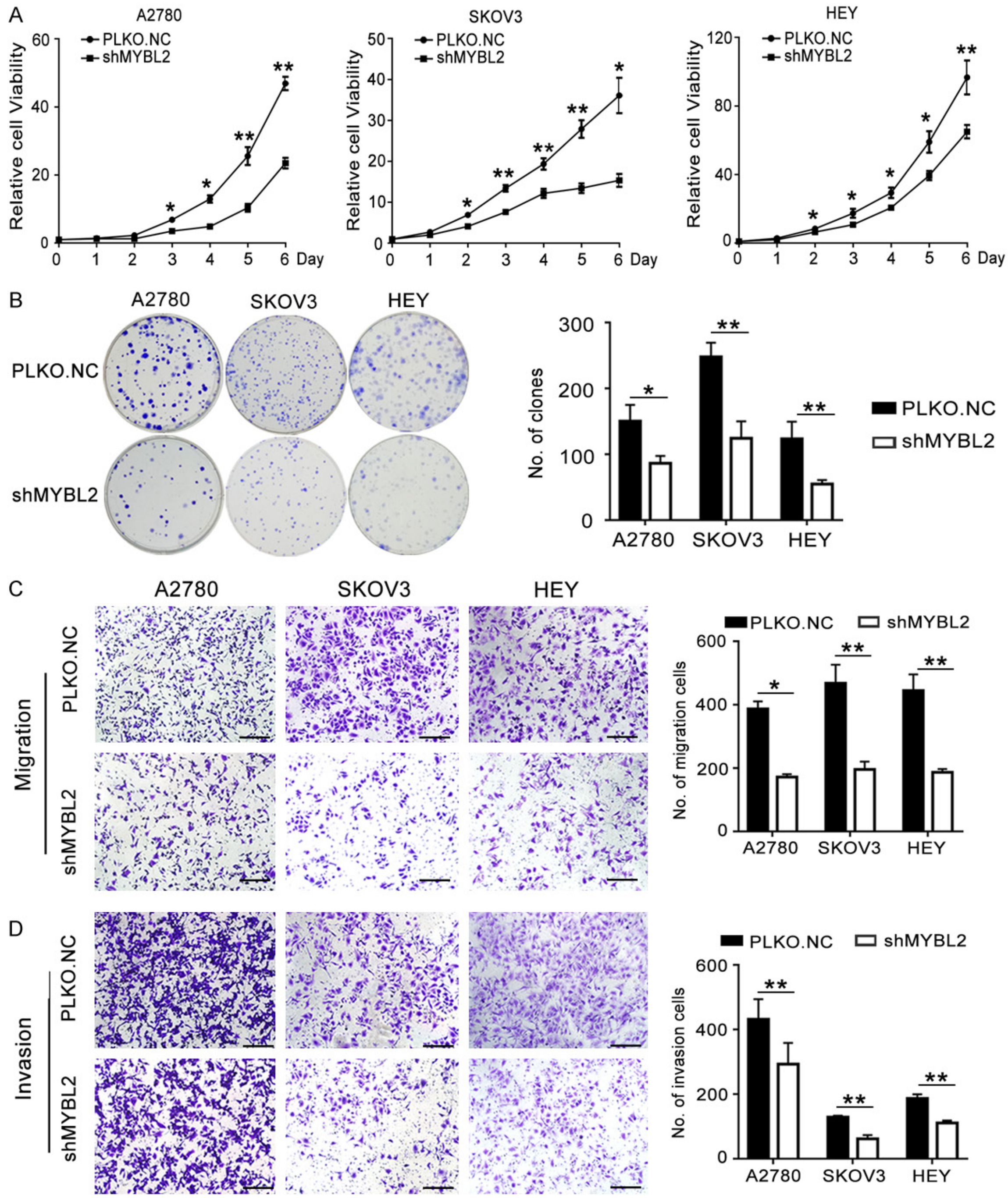

Figure 7. Knockdown of MYBL2 inhibits the proliferation, migration and invasion of ovarian cancer cells. (A) MTT assays were performed to analyze the effect of MYBL2 on cell viability in A2780, SKOV3 and HEY cells. (B) Effect of MYBL2 knocking down on the colony formation of ovarian cancer cells. (C and D) Transwell assays of A2780, SKOV3 and HEY cells after transfection with shMYBL2 or PLKO.NC (200 ×), Scale bar: 50 μm. (Data are mean ± SEM, *P < 0.05, **P < 0.01, n = 3).

Knockdown MYBL2 increases olaparib and cisplatin sensitivity in ovarian cancer cells

To explore the role of MYBL2 in response to olaparib in ovarian cancer cells, HEY and SKOV3 cells were disposed with 40 μM and 100 μM olaparib for 48 h, separately. Western blot assays showed an increased protein level of MYBL2 after olaparib treatment (**Figures 8A**, S2G). Indicated concentrations of olaparib were added to ovarian cancer cells which were stably transfected with PLKO.NC or shMYBL2, and the cell viability was measured by MTT assays 48 h after drug treatment. The shMYBL2 group was more sensitive to olaparib than the control group (**Figure 8B**). The colony formation assays also indicated that ovarian cancer cells with MYBL2 knockdown were more sensitive to olaparib than control cells (**Figure 8C**). As shown in **Figures 8D-F** and S2H, cisplatin treatment elevated the protein level of MYBL2, and knockdown of MYBL2 significantly enhanced the ovarian cancer cells sensitivity to cisplatin.

MYBL2 promotes aggressive tumor behavior dependent on CDCA8

To determine whether MYBL2 increased the aggression of ovarian cancer cells through CDCA8, we performed a rescue experiment. We introduced CDCA8 or PCMV plasmids into HEY cells that were previously transfected with PLKO.NC or shMYBL2. The results showed that MYBL2 knockdown significantly decreased the proliferation and colony formation of HEY cells, whereas ectopic expression of CDCA8 rescued the inhibitory effect induced by shMYBL2 (**Figure 9A**, **9B**). Similarly, the migration and invasion abilities of HEY cells were impaired in the shMYBL2 group, whereas overexpression of CDCA8 rescued the inhibitory effect of shMYBL2 (**Figure 9C**). In addition, we introduced siCDCA8 or NC into SKOV3 cells previously transfected with MYBL2 or PCMV. The results showed that CDCA8 knockdown obviously abrogated the proliferation and metastasis induced by MYBL2 overexpression in SKOV3 cells (**Figure 9D-F**). These results demonstrate that MYBL2 enhanced the aggression of ovarian cancer cells in a CDCA8-dependent manner.

Discussion

CDCA8 has been found to be overexpressed, indicate poor prognosis and participate in the tumorigenesis of several cancers, such as lung cancer [9], breast cancer [8, 20], bladder cancer [18] and cutaneous melanoma [13]. In the present study, we found that the expression of CDCA8 was higher in HGSOC tissues than in FT samples. Moreover, overexpression of CDCA8 promoted the proliferation, migration and invasion of ovarian cancer cells in vitro and accelerated the growth of tumors in vivo.

Inherited and acquired resistance to cisplatin impedes the treatment of ovarian cancer [22]; however, the exact reasons leading to cisplatin resistance remain unclear. Recently, PARPi have displayed exciting effects for the current treatment of ovarian cancers. Moreover, future combined treatment strategies that could enhance the antitumor activity of PARPi are underway [23]. Woong Ju et al. found that CDCA8 was upregulated in chemoresistant epithelial ovarian cancer [24]. Therefore, we hypothesized that CDCA8 may be involved in the chemosensitivity of ovarian cancer to cisplatin and olaparib. In this study, we demonstrated that treatment of ovarian cancer cells with cisplatin and olaparib increased CDCA8 expression and that knockdown of CDCA8 sensitized A2780 and SKOV3 ovarian cancer cells to cisplatin and olaparib.

Previous studies have found that olaparib treatment could cause S or G2/M arrest alone or combined with other drugs [5, 25-29]. In line with this, we found that treating ovarian cancer cells with olaparib at the IC_{50} concentration robustly increased the proportion of cells in G2/M, while combination treatment with CDCA8 knockdown enhanced this effect.

PARPi play roles in cancers by trapping PARP at SSB sites and preventing the repair of SSB, which may be converted to DSB [30], finally leading to cancer cell apoptosis [26]. The rH2AX protein is a widely acknowledged indication of DSB damage [31, 32], and RAD51 is one of the important proteins in the DNA damage response pathway [33]. Our study revealed that silencing CDCA8 increased the sensitivity to olaparib in ovarian cancer depending on increased accumulation of rH2AX and downregulation of the RAD51 accumulation in the nuclei. However, the exact mechanisms by which CDCA8 influences the rH2AX and RAD51 accumulation and the interactions between CDCA8 and other members of the DSB repair pathway still need to be further investigated.

The interaction and regulatory mechanisms of CDCA8 have been investigated. Junn-Liang Chang [34] revealed that CDCA8 interacted and formed a complex with survivin. Satoshi Hayama et al. [9] demonstrated that CDCA8 was coactivated with and phosphorylated/stabilized by AURKB in lung cancer cells. In addition, CDCA8 promoted the progression of cuta-

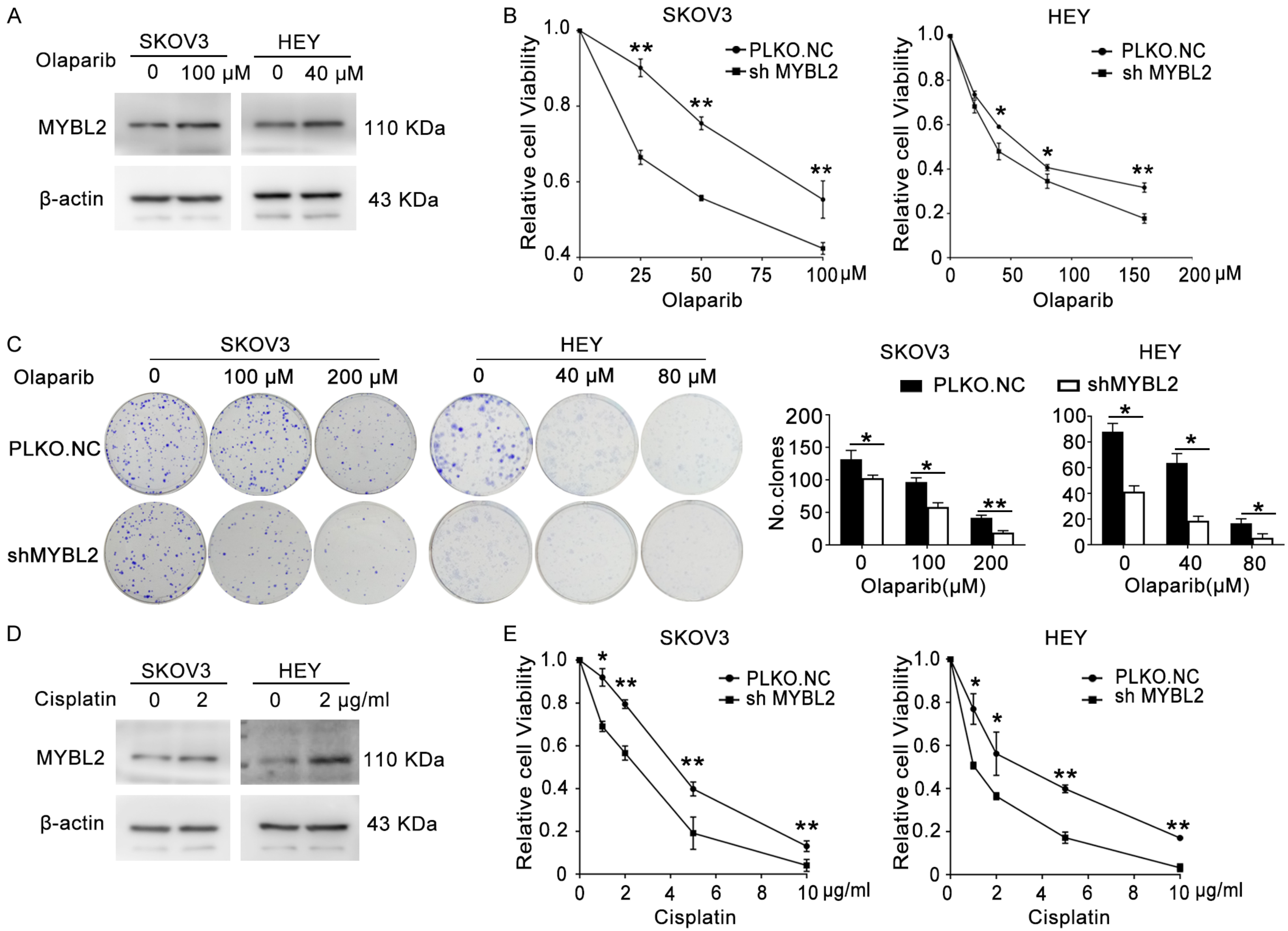
A
Olaparib
SKOV3
HEY
0 100 μM 0 40 μM
MYBL2
110 KDa
β-actin
43 KDa
B
SKOV3
HEY
PLKO.NC
sh MYBL2
Relative cell Viability
Olaparib
C
SKOV3
HEY
Olaparib
0 100 μM 200 μM
0 40 μM 80 μM
PLKO.NC
shMYBL2
No.clones
Olaparib(μM)
D
Cisplatin
0 2
0 2 μg/ml
E
Cisplatin
μg/ml

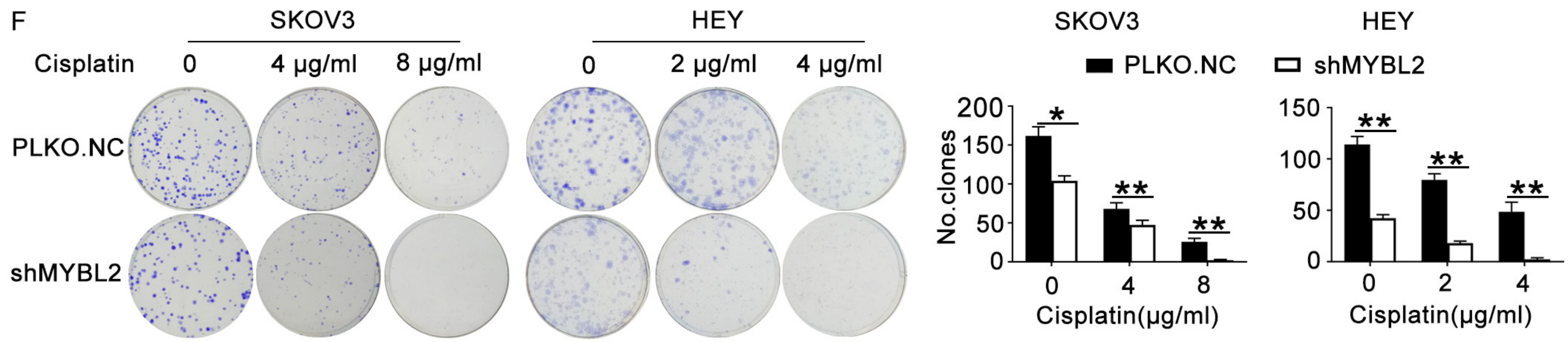

Figure 8. Knockdown MYBL2 increases olaparib and cisplatin sensitivity in ovarian cancer cells. (A) Western blot assay was used to show the protein level of MYBL2 in HEY and SKOV3 cells after treating with 40 μM and 100 μM olaparib. (B and C) The cell viability and colony forming capacity of olaparib treated SKOV3 and HEY cells which were transfected with PLKO.NC or shMYBL2 were detected by MTT assays (B) and colony formation assays (C). (D) SKOV3 and HEY cells were treated with 2 μg/ml cisplatin for 48 h. The protein expression level of MYBL2 was analyzed by Western blot. (E and F) SKOV3 and HEY cells transfected with PLKO.NC or shMYBL2 were treated with cisplatin for 48 h at indicated concentrations. MTT assays (E) and colony formation assays (F) were performed to detect cell viability and colony forming capacity. (Data are mean ± SEM, *P < 0.05, **P < 0.01, n = 3).

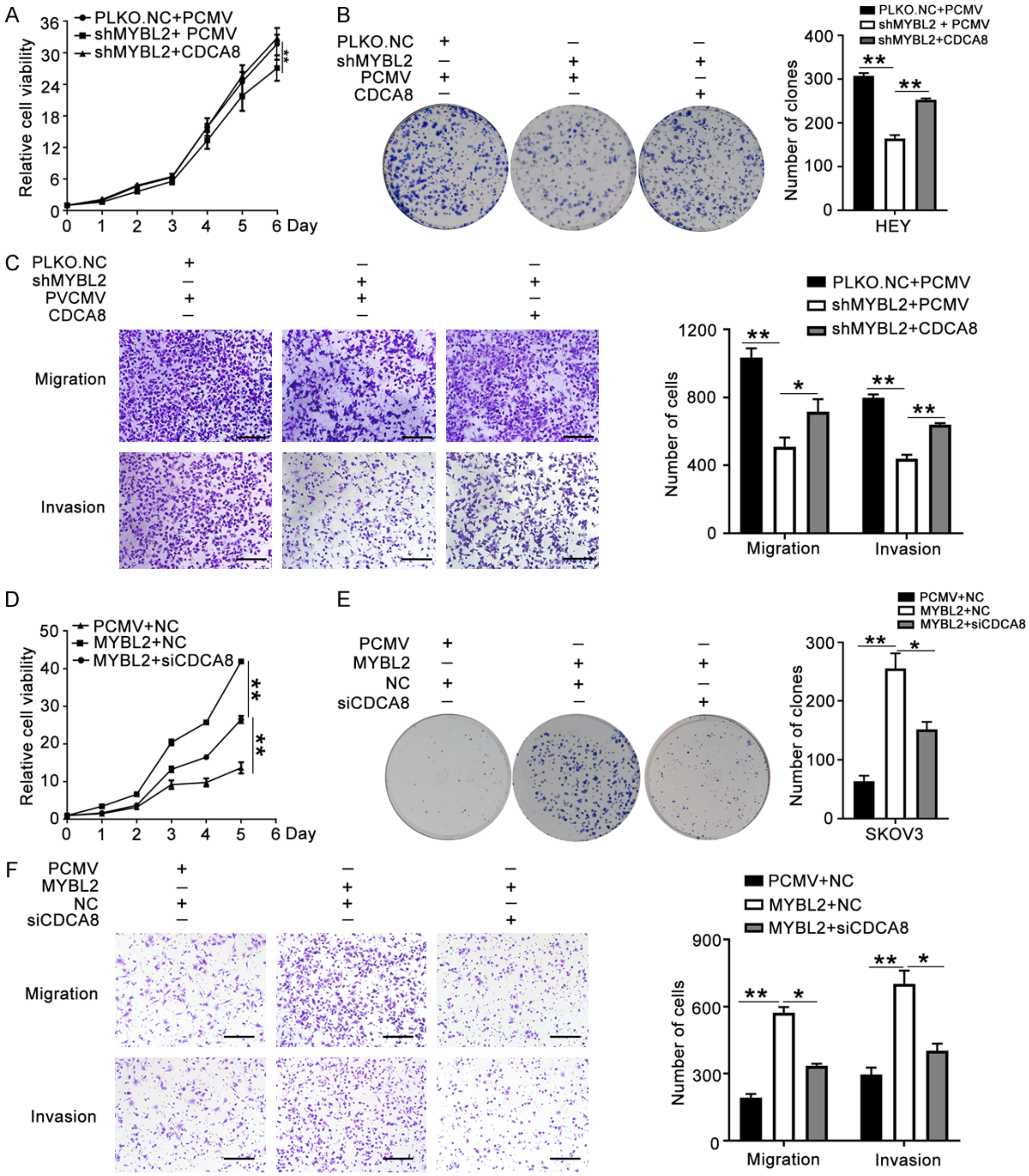

Figure 9. MYBL2 promotes tumor aggressive progression dependent on CDCA8. (A-C) PCMV or CDCA8 plasmids were introduced to HEY cells that transfected with PLKO.NC or shMYBL2. Cell proliferation was detected by MTT assays (A) and colony formation assays (B). Migration and invasion abilities were determined by transwell assays (C) (200 ×), Scale bar: 100 μm. (D-F) MYBL2 over-expressing SKOV3 cells were transfected with siCDCA8 or NC. MTT assays (D), colony formation assays (E) and transwell assays (F) were performed to analyze the effect of CDCA8 depletion on SKOV3 cells stably transfected with MYBL2 (200 ×), Scale bar: 100 μm. (Data are mean ± SEM, *P < 0.05, **P < 0.01, n = 3).

neous melanoma cells via the ROCK pathway [13]. However, few studies have focused on the transcriptional regulation of CDCA8 in ovarian cancer.

The MYBL2 gene belongs to the transcription factor MYB family and has been reported to regulate the cell cycle [35-37], proliferation, survival, differentiation [38] and genome stability maintenance [39-42]. MYBL2, an oncogene, promoted the progression of breast cancer [43], non-small-cell lung cancer [44], gallbladder cancer [45], liver cancer [46] and colorectal cancer [47]. Audra N. Iness et al. reported that the MMB (Myb-MuvB) complex cooperated with FOXM1 to activate G2/M gene expression, and the expression of CDCA8 decreased after the downregulation of MYBL2 in ovarian and breast cancers [35]. Moreover, Rachel Bayley et al. revealed that low MYBL2 levels were associated with the transcriptional deregulation of DNA repair genes [39]. Finally, we hypothesized that CDCA8 might be transcriptionally regulated by MYBL2 in ovarian cancer.

In the current study, we verified that MYBL2 was overexpressed and promoted the progression of ovarian cancer cells. A positive correlation was clarified between MYBL2 and CDCA8 among specimens from ovarian cancer patients. We also illustrated that MYBL2 could bind to the CDCA8 promoter region directly to promote the transcription of CDCA8. Overexpression or knockdown of CDCA8 in MYBL2-depleted or MYBL2-overexpressing cells reversed the effect of MYBL2.

In summary, our study demonstrated that CDCA8 was overexpressed in ovarian cancer tissues. Overexpression of CDCA8 promoted the proliferation, migration and invasion abilities of ovarian cancer cells. Depletion of CDCA8 caused G2/M arrest, increased DNA damage and apoptosis to sensitize ovarian cancer cells to cisplatin and olaparib. In addition, our results illustrated that MYBL2 could promote CDCA8 transcription and act as an oncogene in ovarian cancer dependent on CDCA8. In conclusion, inhibition of CDCA8 combined with cisplatin or olaparib treatment might substantially enhance the therapy of ovarian cancer. We should make efforts to establish methods that can directly and effectively target CDCA8 in the near future.

Acknowledgements

Here, I would like to express my heartfelt thanks to all those who have helped me with this thesis possible and better. This work was financially supported by National Natural Science Foundation of China (81874107, 81902656).

Disclosure of conflict of interest

None.

Address correspondence to: Beihua Kong, Department of Obstetrics and Gynecology, Qilu Hospital, Shandong University, 107 Wenhua Xi Road, Jinan 250012, China. Tel: +86-531-82169269; Fax: +86-531-82169268; E-mail: kongbeihua@sdu.edu.cn

References

[1] Armstrong DK, Alvarez RD, Bakkum-Gamez JN, Barroilhet L, Behbakht K, Berchuck A, Berek JS, Chen LM, Cristea M, DeRosa M, ElNaggar AC, Gershenson DM, Gray HJ, Hakam A, Jain A, Johnston C, Leath CA III, Liu J, Mahdi H, Matei D, McHale M, McLean K, O'Malley DM, Penson RT, Percac-Lima S, Ratner E, Remmenga SW, Sabbatini P, Werner TL, Zsiros E, Burns JL and Engh AM. NCCN guidelines insights: ovarian cancer, version 1.2019. J Natl Compr Canc Netw 2019; 17: 896-909.

[2] Mukherjee A, Huynh V, Gaines K, Reh WA and Vasquez KM. Targeting the high-mobility group box 3 protein sensitizes chemoresistant ovarian cancer cells to cisplatin. Cancer Res 2019; 79: 3185-3191.

[3] Zhong Q, Peng HL, Zhao X, Zhang L and Hwang WT. Effects of BRCA1- and BRCA2-related mutations on ovarian and breast cancer survival: a meta-analysis. Clin Cancer Res 2015; 21: 211-220.

[4] Clements KE, Thakar T, Nicolae CM, Liang X, Wang HG and Moldovan GL. Loss of E2F7 confers resistance to poly-ADP-ribose polymerase (PARP) inhibitors in BRCA2-deficient cells. Nucleic Acids Res 2018; 46: 8898-8907.

[5] Zhong Q, Hu Z, Li Q, Yi T, Li J and Yang H. Cyclin D1 silencing impairs DNA double strand break repair, sensitizes BRCA1 wildtype ovarian cancer cells to olaparib. Gynecol Oncol 2019; 152: 157-165.

[6] Murai J. Targeting DNA repair and replication stress in the treatment of ovarian cancer. Int J Clin Oncol 2017; 22: 619-628.

[7] Lord CJ and Ashworth A. Mechanisms of resistance to therapies targeting BRCA-mutant cancers. Nat Med 2013; 19: 1381-1388.

[8] Phan NN, Wang CY, Li KL, Chen CF, Chiao CC, Yu HG, Huang PL and Lin YC. Distinct expression of CDCA3, CDCA5, and CDCA8 leads to shorter relapse free survival in breast cancer patient. Oncotarget 2018; 9: 6977-6992.

[9] Hayama S, Daigo Y, Yamabuki T, Hirata D, Kato T, Miyamoto M, Ito T, Tsuchiya E, Kondo S and Nakamura Y. Phosphorylation and activation of cell division cycle associated 8 by aurora kinase B plays a significant role in human lung carcinogenesis. Cancer Res 2007; 67: 4113-4122.

[10] Vagnarelli P and Earnshaw WC. Chromosomal passengers: the four-dimensional regulation of mitotic events. Chromosoma 2004; 113: 211-222.

[11] Gu Y, Lu L, Wu L, Chen H, Zhu W and He Y. Identification of prognostic genes in kidney renal clear cell carcinoma by RNAseq data analysis. Mol Med Rep 2017; 15: 1661-1667.
[12] Yan H, Li Z, Shen Q, Wang Q, Tian J, Jiang Q and Gao L. Aberrant expression of cell cycle and material metabolism related genes contributes to hepatocellular carcinoma occurrence. Pathol Res Pract 2017; 213: 316-321.
[13] Ci C, Tang B, Lyu D, Liu W, Qiang D, Ji X, Qiu X, Chen L and Ding W. Overexpression of CDCA8 promotes the malignant progression of cutaneous melanoma and leads to poor prognosis. Int J Mol Med 2019; 43: 404-412.
[14] Kabisch M, Lorenzo Bermejo J, Dünnebier T, Ying S, Michailidou K, Bolla MK, Wang Q, Dennis J, Shah M, Perkins BJ, Czene K, Darabi H, Eriksson M, Bojesen SE, Nordestgaard BG, Nielsen SF, Flyger H, Lambrechts D, Neven P, Peeters S, Weltens C, Couch FJ, Olson JE, Wang X, Purrington K, Chang-Claude J, Rudolph A, Seibold P, Flesch-Janys D, Peto J, dos-Santos-Silva I, Johnson N, Fletcher O, Nevanlinna H, Muranen TA, Aittomäki K, Blomqvist C, Schmidt MK, Broeks A, Cornelissen S, Hogervorst FB, Li J, Brand JS, Humphreys K, Guénel P, Truong T, Menegaux F, Sanchez M, Burwinkel B, Marmé F, Yang R, Bugert P, González-Neira A, Benitez J, Pilar Zamora M, Arias Perez JI, Cox A, Cross SS, Reed MW, Andrulis IL, Knight JA, Glendon G, Tchatchou S, Sawyer EJ, Tomlinson I, Kerin MJ, Miller N; kConFab Investigators; Australian Ovarian Cancer Study Group, Haiman CA, Schumacher F, Henderson BE, Le Marchand L, Lindblom A, Margolin S, Hooning MJ, Hollestelle A, Kriege M, Koppert LB, Hopper JL, Southey MC, Tsimiklis H, Apicella C, Slettedahl S, Toland AE, Vachon C, Yannoukakos D, Giles GG, Milne RL, McLean C, Fasching PA, Ruebner M, Ekici AB, Beckmann MW, Brenner H, Dieffenbach AK, Arndt V, Stegmaier C, Ashworth A, Orr N, Schoemaker MJ, Swerdlow A, García-Closas M, Figueroa J, Chanock SJ, Lissowska J, Goldberg MS, Labrèche F, Dumont M, Winqvist R, Pylkäs K, Jukkola-Vuorinen A, Grip M, Brauch H, Brüning T, Ko YD; GENICA Network, Radice P, Peterlongo P, Scuvera G, Fortuzzi S, Bogdanova N, Dörk T, Mannermaa A, Kataja V, Kosma VM, Hartikainen JM, Devilee P, Tollenaar RA, Seynaeve C, Van Asperen CJ, Jakubowska A, Lubinski J, Jaworska-Bieniek K, Durda K, Zheng W, Shrubsole MJ, Cai Q, Torres D, Anton-Culver H, Kristensen V, Bacot F, Tessier DC, Vincent D, Luccarini C, Baynes C, Ahmed S, Maranian M, Simard J, Chenevix-Trench G, Hall P, Pharoah PD, Dunning AM, Easton DF and Hamann U. Inherited variants in the inner centromere protein (INCENP) gene of the chromosomal passenger complex contribute to the susceptibility of ER-negative breast cancer. Carcinogenesis 2015; 36: 256-271.
[15] Chen YJ, Chen CM, Twu NF, Yen MS, Lai CR, Wu HH, Wang PH and Yuan CC. Overexpression of Aurora B is associated with poor prognosis in epithelial ovarian cancer patients. Virchows Arch 2009; 455: 431-440.
[16] He X, Yang K, Wang H, Chen X, Wu H, Yao L and Ma S. Expression and clinical significance of survivin in ovarian cancer: a meta-analysis. PLoS One 2018; 13: e0194463.
[17] Sui L, Dong Y, Ohno M, Watanabe Y, Sugimoto K and Tokuda M. Survivin expression and its correlation with cell proliferation and prognosis in epithelial ovarian tumors. Int J Oncol 2002; 21: 315-20.
[18] Bi Y, Chen S, Jiang J, Yao J, Wang G, Zhou Q and Li S. CDCA8 expression and its clinical relevance in patients with bladder cancer. Medicine (Baltimore) 2018; 97: e11899.
[19] Bu Y, Shi L, Yu D, Liang Z and Li W. CDCA8 is a key mediator of estrogen-stimulated cell proliferation in breast cancer cells. Gene 2019; 703: 1-6.
[20] Jiao DC, Lu ZD, Qiao JH, Yan M, Cui SD and Liu ZZ. Expression of CDCA8 correlates closely with FOXM1 in breast cancer: public microarray data analysis and immunohistochemical study. Neoplasma 2015; 62: 464-469.
[21] Ju W, Yoo BC, Kim IJ, Kim JW, Kim SC and Lee HP. Identification of genes with differential expression in chemoresistant epithelial ovarian cancer using high-density oligonucleotide microarrays. Oncol Res 2009; 18: 47-56.
[22] Bélanger F, Fortier E, Dubé M, Lemay JF, Buisson R, Masson JY, Elsherbiny A, Costantino S, Carmona E, Mes-Masson AM, Wurtele H and Drobetsky E. Replication protein a availability during DNA replication stress is a major determinant of cisplatin resistance in ovarian cancer cells. Cancer Res 2018; 78: 5561-5573.
[23] Liu J and Matulonis UA. New strategies in ovarian cancer: translating the molecular complexity of ovarian cancer into treatment advances. Clin Cancer Res 2014; 20: 5150-5156.
[24] Ju W, Yoo BC, Kim IJ, Kim JW, Kim SC and Lee HP. Identification of genes with differential expression in chemoresistant epithelial ovarian cancer using high-density oligonucleotide microarrays. Oncol Res 2009; 18: 47-56.
[25] Fang Y, McGrail DJ, Sun C, Labrie M, Chen X, Zhang D, Ju Z, Vellano CP, Lu Y, Li Y, Jeong KJ, Ding Z, Liang J, Wang SW, Dai H, Lee S, Sahni N, Mercado-Uribe I, Kim TB, Chen K, Lin SY, Peng G, Westin SN, Liu J, O'Connor MJ, Yap TA and Mills GB. Sequential therapy with PARP and WEE1 inhibitors minimizes toxicity while maintaining efficacy. Cancer Cell 2019; 35: 851-867, e857.

[26] Zheng F, Zhang Y, Chen S, Weng X, Rao Y and Fang H. Mechanism and current progress of Poly ADP-ribose polymerase (PARP) inhibitors in the treatment of ovarian cancer. Biomed Pharmacother 2020; 123: 109661.

[27] Caracciolo D, Scionti F, Juli G, Altomare E, Golino G, Todoerti K, Grillone K, Riillo C, Arbitrio M, Iannone M, Morelli E, Amodio N, Di Martino MT, Rossi M, Neri A, Tagliaferri P and Tassone P. Exploiting MYC-induced PARPness to target genomic instability in multiple myeloma. Haematologica 2021; 106: 185-195.

[28] Mesquita KA, Alabdullah M, Griffin M, Toss MS, Fatah TMAA, Alblihy A, Moseley P, Chan SYT, Rakha EA and Madhusudan S. ERCC1-XPF deficiency is a predictor of olaparib induced synthetic lethality and platinum sensitivity in epithelial ovarian cancers. Gynecol Oncol 2019; 153: 416-424.

[29] Kim H, George E, Ragland R, Rafail S, Zhang R, Krepler C, Morgan M, Herlyn M, Brown E and Simpkins F. Targeting the ATR/CHK1 axis with PARP inhibition results in tumor regression in *BRCA*-Mutant ovarian cancer models. Clin Cancer Res 2017; 23: 3097-3108.

[30] Strom CE, Johansson F, Uhlen M, Szigyarto CA, Erixon K and Helleday T. Poly (ADP-ribose) polymerase (PARP) is not involved in base excision repair but PARP inhibition traps a single-strand intermediate. Nucleic Acids Res 2011; 39: 3166-3175.

[31] Kuo LJ and Yang LX. Gamma-H2AX - a novel biomarker for DNA double-strand breaks. In Vivo 2008; 22: 305-309.

[32] Matsuda Y, Wakai T, Kubota M, Osawa M, Takamura M, Yamagiwa S, Aoyagi Y, Sanpei A and Fujimaki S. DNA damage sensor gamma-H2AX is increased in preneoplastic lesions of hepatocellular carcinoma. ScientificWorldJournal 2013; 2013: 597095.

[33] Sun C, Yin J, Fang Y, Chen J, Jeong KJ, Chen X, Vellano CP, Ju Z, Zhao W, Zhang D, Lu Y, Meric-Bernstam F, Yap TA, Hattersley M, O'Connor MJ, Chen H, Fawell S, Lin SY, Peng G and Mills GB. BRD4 inhibition is synthetic lethal with PARP inhibitors through the induction of homologous recombination deficiency. Cancer Cell 2018; 33: 401-416, e408.

[34] Chang JL, Chen TH, Wang CF, Chiang YH, Huang YL, Wong FH, Chou CK and Chen CM. Borealin/Dasra B is a cell cycle-regulated chromosomal passenger protein and its nuclear accumulation is linked to poor prognosis for human gastric cancer. Exp Cell Res 2006; 312: 962-973.

[35] Iness AN, Felthousen J, Ananthapadmanabhan V, Sesay F, Saini S, Guiley KZ, Rubin SM, Dozmorov M and Litovchick L. The cell cycle regulatory DREAM complex is disrupted by high expression of oncogenic B-Myb. Oncogene 2019; 38: 1080-1092.

[36] Pilkinton M, Sandoval R, Song J, Ness SA and Colamonici OR. Mip/LIN-9 regulates the expression of B-Myb and the induction of cyclin A, cyclin B, and CDK1. J Biol Chem 2007; 282: 168-175.

[37] Knight AS, Notaridou M and Watson RJ. A Lin-9 complex is recruited by B-Myb to activate transcription of G2/M genes in undifferentiated embryonal carcinoma cells. Oncogene 2009; 28: 1737-1747.

[38] Musa J, Aynaud MM, Mirabeau O, Delattre O and Grunewald TG. MYBL2 (B-Myb): a central regulator of cell proliferation, cell survival and differentiation involved in tumorigenesis. Cell Death Dis 2017; 8: e2895.

[39] Bayley R, Blakemore D, Cancian L, Dumon S, Volpe G, Ward C, Almaghrabi R, Gujar J, Reeve N, Raghavan M, Higgs MR, Stewart GS, Petermann E and Garcia P. MYBL2 supports DNA Double strand break repair in hematopoietic stem cells. Cancer Res 2018; 78: 5767-5779.

[40] Garcia P and Frampton J. The transcription factor B-Myb is essential for S-phase progression and genomic stability in diploid and polyploid megakaryocytes. J Cell Sci 2006; 119: 1483-1493.

[41] Lorvellec M, Dumon S, Maya-Mendoza A, Jackson D, Frampton J and Garcia P. B-Myb is critical for proper DNA duplication during an unperturbed S phase in mouse embryonic stem cells. Stem Cells 2010; 28: 1751-1759.

[42] Shepard JL, Amatruda JF, Stern HM, Subramanian A, Finkelstein D, Ziai J, Finley KR, Pfaff KL, Hersey C, Zhou Y, Barut B, Freedman M, Lee C, Spitsbergen J, Neuberg D, Weber G, Golub TR, Glickman JN, Kutok JL, Aster JC and Zon LI. A zebrafish bmyb mutation causes genome instability and increased cancer susceptibility. Proc Natl Acad Sci U S A 2005; 102: 13194-13199.

[43] Chen J and Chen X. MYBL2 is targeted by miR-143-3p and regulates breast cancer cell proliferation and apoptosis. Oncol Res 2018; 26: 913-922.

[44] Xiong YC, Chen T, Yang XB, Deng CL, Ning QL, Quan R and Yu XR. Overexpression of MYBL2 promotes proliferation and migration of non-small-cell lung cancer via upregulating NCAPH. Mol Cell Biochem 2020; 468: 185-193.

[45] Liang HB, Cao Y, Ma Q, Shu YJ, Wang Z, Zhang F, Ye YY, Li HF, Xiang SS, Song XL, Xu Y, Zhang YC, Bao RF, Yuan RY, Zhang YJ, Hu YP, Jiang L, Li ML, Wang XA, Wu XS, Wu WG, Zhao S, Fand Y, Cui XP, Lu YS, Zhou J, Zheng L, Gong W and Liu YB. MYBL2 is a potential prognostic marker that promotes cell proliferation in gallbladder

cancer. Cell Physiol Biochem 2017; 41: 2117-2131.
[46] Wei T, Weiler SME, Tóth M, Sticht C, Lutz T, Thomann S, De La Torre C, Straub B, Merker S, Ruppert T, Marquardt J, Singer S, Gretz N, Schirmacher P and Breuhahn K. YAP-dependent induction of UHMK1 supports nuclear enrichment of the oncogene MYBL2 and proliferation in liver cancer cells. Oncogene 2019; 38: 5541-5550.
[47] Ren F, Wang L, Shen X, Xiao X, Liu Z, Wei P, Wang Y, Qi P, Shen C, Sheng W and Du X. MYBL2 is an independent prognostic marker that has tumor-promoting functions in colorectal cancer. Am J Cancer Res 2015; 5: 1542-1552.

Table S1. Primer sequences used for PCR

Primer sequences used for qPCR	
Gene	Primer sequences (5' to 3')
β-actin-F	CATGTACGTTGCTATCCAGGC
β-actin-R	CTCCTTAATGTCACGCACGAT
CDCA8-F	CAGTGACTTGCAGAGGCACAGT
CDCA8-R	CTCATTTGTGGGTCCGTATGCTG
MYBL2-F	CACCAGAAACGAGCCTGCCTTA
MYBL2-R	CTCAGGTCACACCAAGCATCAG
RAD51-F	TCTCTGGCAGTGATGTCCTGGA
RAD51-R	TAAAGGGCGGTGGCACTGTCTA
BRCA2-F	GGCTTCAAAAAGCACTCCAGATG
BRCA2-R	GGATTCTGTATCTCTTGACGTTCC
BLM-F	GGTGATAAGACTGACTCAGAAGC
BLM-R	AACGTGCCAAGAGCTTCCTCTC
EME1-F	CTGAACCGAGTCAGCCTGGAAA
EME1-R	GCACCTGTATGTCTGCGAGCAA
BRCA1-F	CTGAAGACTGCTCAGGGCTATC
BRCA1-R	AGGGTAGCTGTTAGAAGGCTGG
RFC3-F	CCTGAGACAGATTGGGAGGTGT
RFC3-R	AGCTCATACAGCCTTCCACGAAC
POLD3-F	TGAGCCTGAACCTCCTTCTGTC
POLD3-R	CTGTGCAGGATTCACTCTCGTAG
POLE2-F	TGCGTCCGTTTTCCTAGCAGCA
POLE2-R	GGGCAGACATAAAGAGGTAGGG
FEN1-F	ACTAAGCGGCTGGTGAAGGTCA
FEN1-R	GCAGCATAGACTTTGCCAGCCT
MCM7-F	GCCAAGTCTCAGCTCCTGTCAT
MCM7-R	CCTCTAAGGTCAGTTCTCCACTC
MCM2-F	TGCCAGCATTGCTCCTTCCATC
MCM2-R	AAACTGCGACTTCGCTGTGCCA
XRCC2-F	TCTGTTTGCTGATGAAGATTCACC
XRCC2-R	CATCGTGCTGTTAGGTGATAAAGC
RAD54L-F	CCCTTTCTTCCATCACCTCGCT
RAD54L-R	GCCTTAGAGCTGTAACCAGGAG
CCNA2-F	CTCTACACAGTCACGGGACAAAG
CCNA2-R	CTGTGGTGCTTTGAGGTAGGTC
E2F2-F	CTCTCTGAGCTTCAAGCACCTG
E2F2-R	CTTGACGGCAATCACTGTCTGC
CDK1-F	GGAAACCAGGAAGCCTAGCATC
CDK1-R	GGATGATTCAGTGCCATTTTGCC
E2F1-F	GGACCTGGAAACTGACCATCAG
E2F1-R	CAGTGAGGTCTCATAGCGTGAC
CCNB1-F	GACCTGTGTCAGGCTTTCTCTG
CCNB1-R	GGTATTTTGGTCTGACTGCTTGC
PLK1-F	GCACAGTGTCAATGCCTCCAAG
PLK1-R	GCCGTACTTGTCCGAATAGTCC
PTTG1-F	GCTTTGGGAACTGTCAACAGAGC
PTTG1-R	CTGGATAGGCATCATCTGAGGC

CDKN1A-F	AGGTGGACCTGGAGACTCTCAG
CDKN1A-R	TCCTCTTGGAGAAGATCAGCCG
MDM2-F	TGTTTGGCGTGCCAAGCTTCTC
MDM2-R	CACAGATGTACCTGAGTCCGATG
TP73-F	CATGGAGACGAGGACACGTACT
TP73-R	TGCCGATAGGAGTCCACCAGTG
TP53I3-F	CACCAGTTTGCTGAGGTCTAGG
TP53I3-R	CCTGGATTTCGGTCACTGGGTA

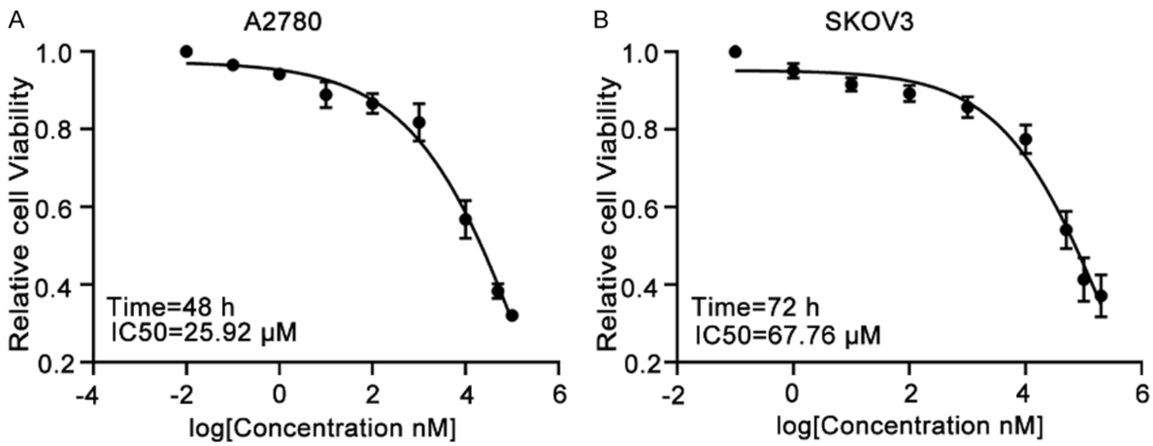

Figure S1. Dose response curve of olaparib in A2780 and SKOV3 cells. (A) Dose response curve of olaparib in A2780. (B) Dose response curve of olaparib in SKOV3 cells.

Table S2. Differentially expressed genes between si CDCA8 and NC

Gene_symbol	adj.*P*.Val	log2FC	fold change
MEGF6	1.39E-19	2.382724514	5.215206991
EMP2	1.31E-11	-1.548972086	0.341753475
RTKN2	1.60E-09	-1.756598976	0.295945007
MELK	1.25E-11	-1.145884296	0.451912605
KLRG2	6.23E-15	3.039595664	8.222605786
EPAS1	5.67E-12	2.516965861	5.723770636
TAF11L12	1.31E-27	3.797573058	13.90539727
CYP21A2	2.73E-12	3.816549005	14.08950484
CYP4F2	1.63E-35	4.225581843	18.70797944
ANO7	2.98E-05	-1.890984961	0.269622919
FAM72A	0.000481883	-1.326822961	0.398645155
TPRX1	1.62E-24	4.017017279	16.18984511
PFKFB4	8.12E-13	-1.314079378	0.402182056
PRR36	5.20E-09	-1.721631377	0.303205667
8-Mar	2.11E-13	1.126955604	2.183973883
IQCN	0.000380666	1.24120619	2.363960926
GDF15	9.57E-52	1.877290079	3.673843265
PEX2	0.009466311	-1.327718882	0.398397671
FLT4	7.07E-07	-1.228023806	0.426901813
TSNARE1	2.84E-05	1.145880687	2.212811695
LYAR	1.54E-08	-1.007691216	0.49734152
PCDHGA11	3.79E-05	1.219695054	2.328974839
SORBS1	3.79E-39	4.676611241	25.57409427
MBD3L2	7.37E-77	5.3338365	40.3315375
KSR1	2.57E-09	1.070690361	2.100438233
HIST1H2BC	3.42E-05	1.502538341	2.833407964
FBXO43	1.44E-09	-1.928649241	0.262674992
SLC2A4	1.92E-06	-1.440041442	0.368556717
TRIM49	2.39E-32	5.206879773	36.93405533
EIF4EBP1	2.84E-12	-1.078480947	0.473527151
FANCI	1.67E-21	-1.36402987	0.388495591
SAMD14	0.000140938	-1.110682064	0.463075051
PLK1	7.86E-25	-1.346606744	0.393215816
CHIC1	3.17E-07	1.204209873	2.304110446
WDHD1	3.66E-15	-1.248444046	0.420901908
ATP1A3	0.000462097	-1.373155243	0.386046023
BTBD19	1.88E-07	1.785211414	3.446689683
SYTL1	1.62E-27	1.95424219	3.875123233
SLC47A1	0.000401161	-1.056416498	0.480824896
BRCA1	1.98E-17	-1.792114078	0.288748613
ALDH1A3	2.07E-05	1.642606317	3.122293841
SLC6A4	2.89E-06	1.9529851	3.871748119
CACNA1G	0.003025073	-1.024196265	0.491684143
CYP2S1	9.91E-05	1.002800964	2.003886732
PDE11A	0.000390135	-1.475058603	0.359718783
KNL1	5.05E-20	-1.361346286	0.389218911
PDGFB	0.000482726	1.015555481	2.021681151

SASS6	2.72E-13	-1.33338019	0.396837374
TAP1	3.99E-16	1.117853117	2.170237778
MGAT5B	1.80E-10	1.88728517	3.699384277
TMEM63B	5.16E-47	1.702863744	3.255465261
RAD51	2.46E-08	-1.277341442	0.412555053
CCNB2	6.37E-24	-1.521325307	0.348365749
SKA3	4.12E-08	-1.152935861	0.449709149
MASP2	0.000208009	1.222310095	2.333200187
ZYG11A	0.00053397	-1.084363077	0.471600425
MAGEB6	2.60E-07	2.149392151	4.436408309
PRAMEF15	1.49E-16	4.491311694	22.49155798
PRAMEF9	3.38E-21	4.656441577	25.21904216
ZNF750	9.97E-22	2.468707524	5.535476549
SECTM1	1.56E-05	1.416725377	2.669788352
GAS2L3	3.71E-07	-1.680986267	0.311869362
MCM4	3.48E-18	-1.077487895	0.473853206
TRIM49D2	1.69E-99	5.422519176	42.88850658
KIF24	7.91E-08	-1.290850573	0.408709994
ARAP1	1.04E-23	1.266788918	2.406253964
ZNF79	1.49E-20	1.871038372	3.65795765
C22orf23	1.58E-12	1.678472528	3.200888734
PCDHGB5	7.39E-05	1.857532437	3.623873103
TMEM56-RWDD3	0.006496242	1.143704304	2.209476066
CDCA8	1.23E-30	-1.938778327	0.260837223
NPNT	2.19E-11	2.011774723	4.032780053
NINJ1	4.69E-19	1.321698709	2.499602536
PLD5	7.80E-28	3.850031187	14.42031913
PRIMPOL	0.0006942	-1.052656344	0.482079724
CHAC1	0.000541111	-1.105939907	0.464599689
ZNF223	1.24E-06	1.596610743	3.024319886
LCN15	0.004172078	1.163981385	2.240749516
MRAP2	0.008066759	-1.146963045	0.451574822
PNP	8.32E-42	1.848277818	3.600701036
CD82	1.92E-13	2.111059069	4.320083116
PRKAB1	2.16E-22	1.518995118	2.865913604
DIAPH3	6.61E-10	-1.3415535	0.394595525
TRIB3	1.24E-05	-1.033484603	0.488528758
SHC1	6.18E-24	1.122084626	2.176612556
DDR1	3.58E-19	1.081708647	2.11654131
TRIML2	1.52E-05	1.840425937	3.581157417
FRZB	5.44E-09	2.493025314	5.62957228
SGO1	9.70E-10	-1.462124115	0.362958343
AUTS2	0.007129408	1.084396291	2.120487959
MIS18A	1.82E-05	-1.030300188	0.489608263
FIGNL1	1.43E-05	-1.097049508	0.467471557
TNFRSF6B	0.001699479	-1.155804843	0.448815734
AL365232.1	2.95E-16	7.518299156	183.3300101
ADAMTSL4	1.14E-07	-1.141606008	0.453254733
CLDN4	0.000695412	1.290825203	2.446679624

FAM84B	3.97E-16	1.737568222	3.334725991
PLCD1	3.64E-17	1.568497808	2.96595726
HIST2H2BE	8.30E-05	1.216727519	2.324189205
CENPJ	8.49E-13	-1.224382183	0.427980751
PCDHGA6	3.67E-05	1.08905083	2.127340296
TERT	6.42E-11	-1.512557383	0.350489376
MATK	0.000178937	-1.366426727	0.38785069
RPL39L	2.55E-07	-1.212451523	0.4315347
UHRF1	1.21E-12	-1.012005825	0.495856363
ARHGAP11A	1.06E-08	-1.052051932	0.482281731
PRR29	0.002864172	-1.210367687	0.432158461
C4B	8.50E-19	2.450472652	5.465951476
CDK1	1.78E-18	-1.254347044	0.419183244
PGM1	5.97E-12	-1.004202991	0.498545474
ITGB3BP	3.63E-08	-1.28777654	0.409581785
ABCA1	1.82E-19	1.30656232	2.473514436
HIST2H3C	0.001939538	1.399254789	2.637653014
SPAG5	1.39E-17	-1.208182835	0.432813428
ARHGAP19	1.71E-10	-1.043695317	0.485083389
LCAT	1.44E-05	1.123252895	2.178375852
CENPK	0.000547077	-1.167750617	0.445114802
TMED7-TICAM2	0.000262417	-1.042894441	0.485352746
GAS6	1.64E-19	2.342809415	5.072895407
CLSPN	5.73E-16	-1.379670244	0.384306626
RRAD	9.99E-07	2.172645142	4.508492564
PRC1	1.30E-05	-1.06255938	0.478781934
SNX32	1.21E-11	2.788364819	6.908463216
SSU72P2	1.16E-85	5.798354493	55.65172469
IQGAP3	1.91E-27	-1.612515303	0.327027689
ZNF730	2.57E-09	-1.80171613	0.286833189
STX16	1.44E-20	-1.320495805	0.400397312
PXT1	1.38E-06	1.86242065	3.636172519
FAM13B	3.73E-22	1.54737738	2.922853218
BRIP1	1.42E-15	-1.205762705	0.433540085
ATP8A2	8.45E-19	3.875579253	14.67795682
SESN2	4.18E-25	1.297541302	2.45809607
PLTP	4.44E-41	2.157152947	4.460337712
F2R	4.40E-05	1.718967021	3.292006128
BTBD10	3.51E-11	1.101852904	2.146301727
STAG3	2.52E-05	1.020933221	2.029231162
KLLN	9.17E-05	1.104198136	2.149793572
CREBRF	1.78E-08	1.200823009	2.298707671
DLGAP5	1.19E-27	-1.599899148	0.329900039
HAP1	0.001095229	1.285588592	2.437814907
LRGUK	0.009294582	1.054764892	2.07737964
SLC26A1	5.37E-05	1.138923286	2.202166096
LY6G5B	0.001882004	1.328656561	2.511686774
P2RX6	0.000325049	-1.332821776	0.396991005
TRIM3	2.74E-23	1.797906466	3.4771528

CCNB1	1.10E-14	-1.115235664	0.461615744
ROM1	0.002116597	1.053441245	2.075474555
DUSP8	9.35E-07	1.89148966	3.710181232
SRGAP3	1.58E-10	1.526077576	2.880017496
OIP5	2.03E-05	-1.363885984	0.388534339
PCDHGC4	0.004187791	1.03008638	2.04214652
CD79B	0.002637265	1.066393491	2.094191671
PRAMEF2	1.93E-37	5.589742901	48.15931281
GTSE1	1.95E-20	-1.387620357	0.382194691
NTPCR	2.63E-11	1.119515171	2.172739437
CATSPERG	1.63E-11	1.954239505	3.875116019
NOTCH1	3.68E-22	1.250878609	2.379863138
ANXA4	3.31E-19	1.323905265	2.503428523
DIRC2	3.71E-07	1.125738373	2.182131998
C14orf28	4.08E-06	1.296560187	2.456424993
CHAF1A	4.07E-15	-1.086544807	0.470887781
KIF15	2.63E-11	-1.470720824	0.360801984
PLB1	2.25E-11	2.24670279	4.74596937
SCN4B	5.24E-17	2.252935354	4.766516708
CENPF	1.45E-31	-1.321883194	0.400012449
PSRC1	4.97E-06	-1.025075958	0.491384427
UBE2C	6.54E-21	-1.403163451	0.37809916
SUGCT	0.004629814	1.022656867	2.031657016
GRN	3.93E-29	1.282716578	2.432966706
CDKN2C	3.73E-08	-1.128117857	0.457512207
CENPA	1.29E-13	-1.831013328	0.281067134
SYCE2	3.46E-05	-1.572593314	0.336203509
AP002990.1	4.50E-15	-5.077776616	0.029609899
GRIN3B	4.91E-08	1.299511717	2.461455601
ACBD7	1.38E-06	-1.375744207	0.385353872
P2RX5	0.001335619	-1.365412198	0.388123529
NADSYN1	1.58E-24	1.458528973	2.748279957
AEN	1.79E-13	1.035397999	2.049679017
NTN1	2.55E-26	3.774238102	13.68229278
MCM10	9.58E-19	-1.431033321	0.370865168
ADGRB1	1.14E-05	1.123177934	2.178262669
GINS2	1.58E-09	-1.143249908	0.45273856
FN1	0.001246742	1.340102729	2.531693454
ZNF423	2.91E-10	1.872969648	3.662857684
C3orf14	1.21E-06	-1.870767588	0.273427909
RHOC	9.24E-08	1.008255188	2.011476926
C21orf58	4.05E-13	-1.394668618	0.380332039
KIF11	3.73E-22	-1.357260543	0.39032275
DEPDC1B	1.05E-09	-1.281661201	0.411321617
RAPGEF3	0.00489355	1.204284994	2.304230423
ZBTB4	5.90E-15	1.038032804	2.053425782
HSPB1	0.004475117	1.125610384	2.181938417
NUF2	1.01E-18	-1.788849607	0.289402721
RBM12	2.36E-12	-1.248586106	0.420860464

NIPSNAP3B	0.005711344	-1.286281557	0.410006431
SNAI3	1.17E-11	2.100136255	4.287498763
TAF11L14	9.02E-14	3.949597969	15.45067508
TBC1D9	4.14E-09	1.035098106	2.049252994
NUAK1	5.60E-10	3.132956407	8.772307639
DKK3	0.000713692	2.141285392	4.411549254
TLE6	0.001918975	-1.408430015	0.376721424
HIF3A	0.000212699	-1.32295407	0.399715641
ABTB2	6.77E-19	2.305146281	4.942175631
FLYWCH1	6.97E-13	1.073570441	2.104635566
CD164L2	6.28E-10	3.641117885	12.4762969
HASPIN	4.46E-08	-1.227033597	0.427194922
TMEM254	6.92E-05	1.061558163	2.08718454
TEX37	9.02E-14	3.731302682	13.28109949
TSPAN12	0.000969773	-1.135758619	0.455095549
PTCHD4	1.72E-09	1.993808021	3.982868979
FBXO44	1.55E-18	1.300355928	2.462896374
MGRN1	9.92E-06	1.099932807	2.143447092
DISC1	0.000980633	-1.030007343	0.489707656
HAT1	2.33E-14	-1.066558698	0.477456533
HIST1H2BD	0.001563734	1.128315153	2.186032959
ZNF337	1.47E-14	1.131831362	2.191367367
FAM72C	5.42E-13	-1.957744262	0.25743065
LPIN3	1.04E-26	1.439492418	2.712254237
TTLL7	5.42E-06	-1.169720852	0.44450734
AREG	6.08E-06	1.910904909	3.760448942
BTG2	8.95E-13	2.573934129	5.954309151
CARMIL3	0.000179938	-1.347646781	0.392932449
PDE2A	1.67E-12	2.729724902	6.633291387
NRTN	3.80E-05	-1.381607999	0.383790791
SMTN	2.90E-41	1.866200862	3.645712669
PRIMA1	0.002592767	-1.391443498	0.381183216
PPP1R18	0.004642024	1.460551784	2.752136038
TRIM64	2.39E-25	4.312361823	19.86782202
AL109811.3	4.12E-05	1.792831732	3.464943269
RAD18	8.40E-07	-1.018357902	0.493677944
FRMPD2	9.39E-12	3.097323817	8.558297419
EPN3	0.000114547	1.163680398	2.240282082
SUOX	3.89E-19	1.612267716	3.057320326
CSPG5	1.51E-06	-1.610414335	0.32750428
PI15	0.002463905	1.433904518	2.701769351
IDUA	1.93E-11	1.353967691	2.556141481
ATP8B3	6.14E-05	-1.352310433	0.391664308
KHDC1L	3.25E-62	4.624199383	24.66168353
CENPQ	5.32E-06	-1.38660125	0.382464765
SSC4D	3.36E-07	-1.759564883	0.295337226
UNC45B	1.65E-19	3.708343552	13.07141621
VMAC	2.79E-05	1.214671665	2.320879573
PODNL1	4.46E-08	1.668694908	3.179268601

MTURN	9.25E-07	1.355352202	2.558595711
VKORC1	5.69E-09	-1.073068072	0.475307123
EGR2	2.19E-05	1.864951944	3.642557998
C4A	1.98E-24	2.869735296	7.309310374
SNURF	0.005972395	2.576774458	5.966043341
LRRCC1	0.00046049	-1.462924047	0.362757149
FAM104A	2.14E-34	1.596285416	3.02363798
GRIP2	2.41E-15	3.086729151	8.495678381
TINCR	8.10E-18	2.379787294	5.204600017
ZSCAN4	5.99E-75	4.743396686	26.78580383
CASTOR3	1.47E-06	1.272501	2.415799964
UPK1A	1.57E-09	-1.579587395	0.334577563
ZNF284	3.71E-06	1.190264945	2.281946463
VRK1	3.13E-14	-1.50138524	0.35321408
GGT6	0.000203528	2.475850092	5.56294982
KIF18A	3.22E-15	-1.549908217	0.341531792
ZNF28	0.000228672	1.013103545	2.018248115
LOX	2.28E-08	-1.999322168	0.250117487
SERTAD1	1.64E-06	1.174196312	2.256671326
DTL	3.24E-26	-1.493964495	0.355035577
NKX2-5	1.11E-15	1.230461308	2.346420056
C2orf66	0.002876046	1.242800154	2.366574196
JPH1	0.005834531	-1.168951589	0.44474442
AHNAK2	5.09E-18	2.819799364	7.060641974
FOXD4	5.76E-06	1.922027268	3.789551907
APLN	2.82E-09	1.656946024	3.153482713
GJA5	0.000577837	1.190729172	2.282680861
SSU72P5	9.40E-81	6.045124512	66.03342225
SRSF8	8.35E-29	1.714778512	3.282462461
ZGRF1	7.30E-16	-1.629177854	0.323272378
CYP4F3	2.41E-48	5.287058302	39.04479417
TPX2	4.73E-20	-1.122489582	0.459300551
MMS22L	1.49E-07	-1.015324072	0.494717188
ABCG4	6.20E-07	1.408457622	2.654532164
PLXNB2	2.16E-22	1.087488698	2.125038086
CAMK2B	5.50E-05	1.635727228	3.107441492
DEPDC1	7.06E-29	-1.636574439	0.321619227
CCDC15	1.24E-06	-1.629030255	0.323305453
ITM2B	4.51E-20	1.088974107	2.127227166
RADIL	1.48E-05	-1.086890472	0.470774972
SDC4	3.22E-15	1.255267115	2.38711342
RFC3	5.75E-13	-1.220402817	0.429162874
PITX3	0.000535938	-1.500591819	0.353408386
PRELID2	2.56E-08	-1.393953312	0.380520659
EFNB2	4.18E-06	1.719723356	3.293732419
INPP5D	1.73E-45	2.356415032	5.120962634
ADARB1	8.70E-08	1.187184588	2.277079385
FBLN5	4.10E-05	1.083869321	2.119713554
PALM3	5.95E-05	-1.030027141	0.489700936

MFGE8	3.99E-13	1.093603351	2.134063864
NMNAT2	0.001713703	1.401297032	2.641389454
PRAMEF13	8.36E-36	7.193060473	146.3278404
IGDCC4	1.21E-24	1.927392719	3.80367167
STAMBPL1	6.64E-07	-1.653224266	0.317928826
LOXL4	4.56E-09	1.477680382	2.785005897
MCM6	3.27E-16	-1.085831755	0.471120575
RFPL4A	1.23E-91	6.282842886	77.8617511
C12orf45	1.60E-16	1.340017464	2.531543832
PRRT4	0.001990949	-1.353108907	0.391447597
INPP1	0.005711344	1.152328561	2.222723605
ZNF492	0.00572855	-1.059954013	0.479647348
WDR63	1.44E-27	2.228948726	4.687922519
FZD9	5.71E-05	-1.506568957	0.351947232
FEN1	1.02E-10	-1.003275723	0.498866009
PHYHIP	4.06E-09	2.045507166	4.128183686
BRCA2	1.88E-19	-1.467094341	0.361710068
CCM2L	1.64E-05	-1.259383942	0.417722297
KLF18	2.13E-32	5.585928737	48.03215849
ZNF724	8.95E-06	-1.152236544	0.449927189
TBCEL	5.18E-07	1.299372702	2.461218432
WDR76	1.74E-11	-1.426958431	0.371914156
AMOTL1	3.65E-09	1.881613956	3.684870595
XPC	3.83E-24	1.334755579	2.522327449
ATP1B2	6.62E-09	-1.060804969	0.479364518
LPAR3	0.000206854	-1.084520268	0.471549044
PCDHB12	0.001167597	1.134020961	2.194695761
RETSAT	9.79E-11	1.512307942	2.852660268
STAC2	2.67E-08	-1.4274684	0.371782714
DOC2B	0.002241547	-1.438811553	0.368871044
KCTD1	2.24E-09	1.287228382	2.44058734
CEP128	1.24E-07	-1.404862996	0.377654008
TVP23C-CDRT4	0.000972902	1.399413809	2.637943764
BMF	2.75E-06	-1.825634293	0.282117039
ARHGAP33	8.81E-11	-1.560981652	0.338920392
SYTL2	9.46E-08	1.638425799	3.113259423
CHRM4	2.00E-06	-1.974562305	0.254447107
TRPM6	3.32E-10	3.218592349	9.308781596
EFHD1	3.77E-08	-1.452914404	0.365282766
MCM3	3.27E-18	-1.090818393	0.46949497
S1PR3	1.95E-09	2.611125361	6.109800873
HJURP	2.80E-20	-1.545071749	0.342678659
SGO2	5.85E-17	-1.458324476	0.36391553
ICAM1	0.000230701	-1.33090704	0.397518239
PRIM2	6.56E-08	-1.174918508	0.442908777
ARHGEF3	0.000573389	1.075945741	2.108103561
ZBTB8B	0.000157543	-1.336208522	0.396060156
ENG	0.002129701	-1.241463905	0.422943277
KIF14	2.79E-23	-1.424309284	0.372597711

ULK1	3.56E-17	1.196707745	2.292159988
KIF18B	1.97E-18	-1.324411684	0.399311995
PLCL2	2.11E-08	1.604792811	3.041520675
SAT1	2.31E-20	1.835697553	3.56943951
KNSTRN	1.29E-05	-1.009438367	0.496739588
FRMD8	0.001950638	1.053317042	2.075295883
SSU72P3	8.64E-60	6.175025159	72.25498194
RRM2	1.15E-05	-1.144939983	0.452208501
GADD45A	7.30E-19	1.334439183	2.521774341
BRMS1L	4.34E-13	1.293743707	2.451634152
TP53INP1	4.45E-35	1.610966649	3.054564382
SPATA25	2.27E-05	1.830912042	3.557619067
DSN1	3.86E-10	-1.40486063	0.377654628
COL4A5	2.14E-27	1.46747426	2.765373331
AGRN	2.61E-37	1.395848192	2.631432143
DGKZ	2.91E-15	1.066516589	2.094370366
JCAD	1.60E-21	2.086843998	4.248177355
CALML6	0.009290971	1.023187147	2.032403913
LCE1E	4.28E-11	2.894615005	7.436454797
SLCO4A1	0.00160086	-1.161995324	0.446894029
DBF4	2.63E-11	-1.239133566	0.423626996
SOX9	8.84E-05	1.558610282	2.945699536
GRIN2C	3.07E-29	2.470322589	5.541676861
AURKB	2.68E-14	-1.313310963	0.402396326
SCML1	7.72E-05	-1.036067211	0.487655012
EID2B	0.000103085	1.112963735	2.162895158
CAPS	1.38E-05	1.254944233	2.386579232
PRODH	2.49E-12	2.028930047	4.081020754
PSTPIP2	1.22E-21	1.81610563	3.521293863
BAG1	3.02E-10	1.516207461	2.860381269
PDE4C	7.27E-30	1.633591241	3.102844163
RFPL4AL1	1.45E-72	5.676830087	51.15594789
PHF19	1.97E-16	-1.267650873	0.41533551
TRIM32	0.000818873	1.44599875	2.724513708
PIDD1	9.79E-35	1.584730782	2.999518194
RNF19B	4.19E-18	1.355639353	2.559105019
PRAP1	4.81E-34	3.011508245	8.06407046
DDX60	0.000351594	-1.06087716	0.479340532
KDM4E	9.71E-77	5.430911746	43.13872842
STMN1	1.40E-17	-1.104053186	0.465207678
ABHD10	0.001217088	-1.030066274	0.489687653
MBOAT1	0.000557249	-1.415328347	0.374924408
FANCG	1.89E-12	-1.302596089	0.405396043
KIF20B	4.72E-14	-1.10321682	0.465477449
CEP55	2.53E-23	-1.693808148	0.309109918
RNASEH2A	7.91E-13	-1.315156905	0.401881785
LHX3	2.12E-19	5.120963893	34.79875756
EXOSC8	2.69E-12	-1.2838216	0.410706134
DMC1	6.49E-06	-1.579043098	0.334703815

CDKN1A	0.00365932	2.025628747	4.071692885
TP73	2.99E-07	1.696969072	3.242190975
RINL	8.89E-05	1.09730292	2.139543365
VWCE	3.47E-20	2.018294116	4.051045015
COL23A1	6.29E-07	1.247203106	2.373807762
RND1	1.04E-05	1.087167327	2.124564771
MICAL1	2.51E-12	1.118334265	2.170961687
SLF1	1.03E-06	-1.019932416	0.493139453
GDF9	0.00224842	1.124477969	2.18022642
ENO1	1.96E-22	-1.004951894	0.498286746
KLHL41	5.85E-06	-1.419393959	0.373869332
PRAMEF25	1.11E-25	5.004047285	32.0898977
KDM4F	7.09E-17	5.03654832	32.82102341
PXDN	1.33E-24	6.214615359	74.26524779
PODXL	1.53E-05	1.504130081	2.836535818
TTLL6	2.10E-05	1.479148333	2.787841099
PCDHGA10	1.85E-14	1.06933746	2.09846945
TRIM22	1.77E-11	1.856292603	3.620760128
ASTN2	1.71E-13	1.719450969	3.293110606
TCF19	3.46E-05	-1.086762465	0.470816744
CES2	4.72E-09	1.224784696	2.337205672
CENPI	8.59E-09	-1.444474378	0.367426
DRP2	0.003379064	-1.147208979	0.451497849
TRIM64B	3.09E-39	4.667623332	25.41526435
PCSK4	1.78E-05	-1.122090724	0.45942755
REEP6	8.86E-11	-1.504029199	0.352567354
ZNF530	0.001953004	-2.020262797	0.246513268
RAB6B	9.54E-09	1.092345893	2.132204616
PROM2	7.40E-05	1.877652556	3.674766433
PBK	1.35E-19	-1.695216602	0.308808292
PRAMEF14	1.28E-25	4.49734382	22.58579545
PKN3	3.48E-11	-1.119461373	0.460265632
CIT	9.11E-36	-1.761007824	0.295041986
VPS13C	6.08E-23	1.619089262	3.071810592
CCDC116	0.003845021	-1.292843866	0.408145692
CTSV	5.10E-11	-1.352030247	0.39174038
KIF20A	2.63E-20	-1.433824587	0.370148327
FANCB	0.000295727	-1.186135183	0.439478599
AP5Z1	2.64E-09	1.003275391	2.004545815
RNF125	3.26E-05	-1.391246475	0.381235276
PRAMEF26	1.39E-22	5.036122984	32.81134853
C10orf95	0.00708685	-1.131418137	0.456466808
TMEM145	1.25E-07	-1.494646172	0.354867861
AC007906.2	0.000177397	1.183637469	2.271487662
OTP	1.24E-35	4.502895693	22.67287904
KIF22	6.52E-13	-1.023223423	0.492015809
PHLDB3	1.36E-17	1.497145675	2.822836705
REEP2	8.17E-07	1.044939467	2.063279785
CCNA2	4.53E-27	-1.4867086	0.356825692

KIF23	1.34E-18	-1.279380197	0.41197246
NUSAP1	2.96E-44	-2.691644096	0.154786967
RAD54B	1.30E-05	-1.16876562	0.444801753
MOXD1	0.000748237	-1.38892553	0.381849085
BUB1	2.39E-32	-1.60213678	0.329388758
INKA2	1.90E-20	2.109403763	4.315129221
PCYT1B	3.82E-07	-1.353618339	0.391309397
CCR10	2.28E-07	-1.640110545	0.32083189
IFI27L1	0.001636772	-1.020104087	0.493080777
RACGAP1	1.53E-14	-1.195441651	0.436652755
DQX1	1.49E-18	1.912913828	3.765688926
C1QL4	2.81E-06	-1.513277514	0.35031447
AURKA	4.82E-20	-1.371263363	0.386552597
FOXM1	2.16E-06	-1.234070674	0.425116254
GP1BB	0.0053222	2.598773312	6.057713353
EFNA3	1.09E-06	-1.238050856	0.423945038
ASF1B	1.49E-11	-1.17195418	0.443819764
EOMES	0.002147708	1.178892454	2.264029025
CIP2A	4.11E-11	-1.035323637	0.487906417
SHCBP1	2.76E-15	-1.606014612	0.32850458
TUBB3	2.36E-05	-1.127399857	0.457739959
PRAMEF6	5.80E-21	5.48120359	44.66904762
NEXN	4.85E-15	1.411524818	2.660181751
HIST1H2AG	9.93E-05	1.253906259	2.384862781
MUC6	3.80E-18	2.717575503	6.577664858
HHAT	3.34E-18	3.414982377	10.66625913
ABHD4	3.90E-32	1.70051841	3.250177277
TAF13	3.72E-05	1.078838368	2.112334582
LSM11	6.20E-05	-1.050754547	0.482715632
CPNE5	0.000153458	-1.599853527	0.329910471
CLN8	2.76E-09	1.267429478	2.407322585
TPRG1L	1.48E-07	1.232895344	2.350382149
FOSL1	1.35E-06	2.232143277	4.698314461
PRAMEF1	1.31E-34	5.803780306	55.86141861
PRAMEF12	6.42E-45	4.680970913	25.65149336
PRR11	6.90E-16	-1.133378713	0.455846905
PCDHGB3	1.22E-05	1.176745837	2.260662833
C2	0.000235355	1.289615467	2.444628881
ROBO3	0.00041227	-1.102666635	0.465654997
HMGB2	4.72E-28	-1.438935175	0.368839437
MAD2L1	4.18E-23	-1.559147095	0.339351643
SSU72P4	3.69E-116	6.321209359	79.96015474
SPC24	2.68E-18	-1.859563633	0.275559614
PRSS57	1.19E-07	2.274831106	4.839409781
ADAMTS7	4.15E-39	1.701979159	3.253469794
PODN	3.75E-15	2.251135889	4.760575168
CDH3	2.52E-35	3.846163953	14.38171633
TRIP13	3.36E-12	-1.080633898	0.472821027
CEP85L	5.02E-33	1.823660125	3.539781047

MKI67	3.43E-42	-1.586246719	0.333036748
LRP1	1.22E-25	1.130462362	2.189288924
RIC3	0.002178974	1.068371985	2.09706559
CDCA2	7.46E-13	-1.305030518	0.404712547
NXF1	7.82E-24	1.336492541	2.525366085
MYBL2	1.32E-22	-1.318352635	0.400992557
MPZ	0.007053555	1.142239226	2.207233451
ZNF519	4.61E-05	-1.122059103	0.45943762
RALGDS	5.31E-10	1.596193653	3.023445667
PRKX	3.29E-33	1.64149234	3.119883894
PRAMEF20	3.36E-12	3.443555011	10.87961056
ATP23	0.000170368	-1.286792005	0.40986139
ELFN2	4.61E-10	2.489755323	5.616826826
RFC4	2.50E-07	-1.073762555	0.475078376
FSBP	9.25E-07	-1.21814531	0.429834947
TBC1D2	4.95E-07	1.671227434	3.184854432
AC106774.4	7.67E-29	3.987892111	15.86628112
PLPPR4	0.0011713	-1.221090458	0.428958368
H3.Y	1.01E-62	4.709282613	26.15985452
GLS2	1.15E-20	2.198097813	4.588739198
GRIN1	0.000504804	-1.493979645	0.355031849
POLD3	2.10E-13	-1.222692158	0.428482397
CD4	2.82E-05	-1.461931488	0.363006808
ALPG	1.93E-23	3.036993458	8.207787943
NCAPG	1.37E-23	-1.533298156	0.345486644
RAB26	1.06E-06	-1.405953348	0.377368695
COL9A2	9.08E-18	1.865269554	3.643359999
ADGRG1	3.19E-40	3.922473877	15.16290082
BLCAP	1.13E-15	1.193818598	2.287574293
TRIM49B	4.18E-67	5.191272237	36.53664446
PTTG1	1.79E-17	-1.347916051	0.392859118
CCDC77	2.83E-05	-1.119852044	0.460141013
GH2	0.009436066	1.264432501	2.402326932
C17orf80	0.002585529	1.489610376	2.808131266
DENND2C	2.66E-05	1.464601977	2.759873185
ZNF684	0.000781751	-1.232088123	0.42570085
ITGA10	2.32E-05	1.561455347	2.951514331
DUSP13	0.004634519	1.116090647	2.167588122
SAMD11	6.29E-10	-1.45835833	0.363906991
FAM210B	1.32E-49	2.242587374	4.732450363
ESR1	0.005220549	1.589571683	3.009599851
SERPINE1	7.26E-27	1.382258096	2.606760603
IKBIP	1.85E-11	1.037167709	2.052194838
COL15A1	1.00E-29	7.622703103	197.0889529
ADAM19	6.16E-53	2.063730242	4.18065862
DNA2	2.71E-12	-1.280073976	0.411774394
S100A6	0.000751132	1.358483533	2.564155106
GJB5	7.43E-08	2.150626659	4.440206149
HPX	1.48E-17	3.470605393	11.08552655

PCBP4	1.61E-15	1.480946203	2.791317439
PRF1	1.51E-06	1.972683602	3.924975374
EME1	7.33E-06	-1.582650552	0.333867935
JMJD7-PLA2G4B	1.83E-50	4.095783711	17.09833228
PEAR1	7.18E-07	1.904235069	3.743103832
FBXL16	1.86E-06	-1.939152276	0.260769623
ZWINT	1.91E-12	-1.129449999	0.457089949
SLC30A1	5.11E-18	1.598506909	3.02829743
ATAD2	1.20E-26	-1.385329108	0.382802164
TRIM48	1.18E-43	5.112665926	34.59917964
BUB1B	7.47E-27	-1.495810091	0.354581681
CA9	4.37E-08	-2.410746829	0.188058467
TIMELESS	9.89E-15	-1.043425786	0.485174023
LINGO1	6.62E-11	2.18514493	4.547724724
F11R	1.52E-16	1.38187456	2.606067695
YJEFN3	8.59E-09	1.009240684	2.012851422
PLXNB3	5.09E-72	3.151904725	8.888282834
NEURL2	2.41E-05	3.174532889	9.028791454
GABRP	1.26E-12	3.465845211	11.04901006
ZNF596	0.003492758	1.28138545	2.430722922
TMEM127	6.03E-13	1.012851466	2.017895502
DUSP9	6.84E-05	-1.366785854	0.387754155
CDC25C	7.01E-07	-1.459649252	0.363581512
RFC5	3.14E-10	-1.170573991	0.444244558
TRPV4	7.44E-06	-1.058252912	0.480213241
DUOX1	1.13E-08	2.456578768	5.489134798
HSPBAP1	0.000109886	1.00778375	2.01081973
DOCK4	3.61E-06	1.204059934	2.303870993
PARD6G	6.22E-25	1.742763477	3.346756241
ZFPM1	2.18E-08	1.220209462	2.329805408
AC008397.2	1.56E-34	1.941367112	3.840694232
LACC1	0.008578	1.190480081	2.282286775
ACTN3	2.26E-26	-1.500633651	0.353398139
ITGA3	2.95E-49	2.230729501	4.69371258
ASAP2	0.0003966	-1.008061598	0.497213855
HPCAL4	6.66E-05	-1.474755601	0.359794341
LIMK2	4.08E-15	1.120069672	2.173574691
LIPA	5.47E-16	1.111786309	2.161130675
SLC7A8	2.81E-16	1.655197591	3.149663254
CCDC18	7.08E-08	-1.125875762	0.458223781
SLC13A3	0.000177905	1.003534405	2.004905732
CUL4B	3.52E-17	-1.262475267	0.416828184
SPATC1L	0.000425028	-1.563432493	0.338345125
FOXS1	6.36E-09	1.581641324	2.99310175
LAMC1	4.90E-22	1.001808276	2.002508375
TNK1	7.89E-05	1.423153537	2.681710565
WDR62	2.25E-13	-1.173546632	0.443330145
TRPM2	3.06E-19	3.052426353	8.296060145
AL662899.2	5.92E-05	1.054369094	2.076809797

FANCA	1.03E-13	-1.260901053	0.417283259
CUL9	8.91E-17	2.443956665	5.441319965
OLFML2A	5.84E-07	-1.241943992	0.422802557
SORCS2	7.32E-10	2.968347305	7.826391636
HSPA4L	8.41E-14	1.115866156	2.16725086
ZNF385A	2.34E-16	1.105733129	2.152082118
MBD3L5	3.16E-58	5.860080382	58.08446212
OLFML3	0.000144436	1.113963789	2.164394963
CRISPLD2	2.48E-27	3.591353906	12.05328014
CFAP221	0.00404686	-1.140341847	0.453652072
NOSTRIN	0.001788162	-1.319978267	0.400540972
SLC39A13	3.63E-07	1.240352397	2.362562339
MEIOB	6.95E-06	-1.071846789	0.475709655
MGAT4A	0.006787227	-1.262967249	0.416686063
NRGN	2.96E-07	-1.126230414	0.458111151
SMIM13	5.62E-08	-1.340863921	0.394784179
GGH	2.48E-10	-1.507463455	0.351729085
TRIM43B	4.42E-92	6.245695054	75.88248678
TRIM43	6.61E-101	6.342669621	81.15846206
ASPM	7.97E-37	-1.59194139	0.331724761
MAN2B1	1.86E-17	1.066767869	2.094735182
FLG2	0.001658889	1.080083364	2.114158242
ABCG2	0.007388821	1.09279084	2.132862319
DGKA	3.78E-10	1.087582838	2.125176755
ZNF440	4.41E-07	1.048201747	2.067950635
PIGX	2.81E-08	-1.363909922	0.388527892
PNMA2	0.000386578	-1.025302207	0.491307372
NEK2	5.54E-23	-1.779230082	0.291338833
HAGHL	0.000470657	-1.065941654	0.477660786
HIST2H3A	0.002732396	1.351048697	2.550974888
TNFRSF14	2.25E-09	1.642627139	3.122338905
REXO5	8.17E-07	-1.300600153	0.405957287
SLC4A8	0.000963049	1.231377719	2.347910994
SOWAHA	0.003388036	-1.253112841	0.419542003
ORC1	2.89E-14	-1.354373947	0.391104503
EFNA4	0.000107655	-1.123552094	0.458962411
C1QL1	4.37E-05	-1.190467748	0.438160778
C19orf57	0.000868611	-1.286973151	0.40980993
FITM2	6.70E-06	1.042175363	2.059330469
PTK2B	3.70E-07	1.192736098	2.285858497
GRHL3	1.58E-47	3.236405792	9.424432786
PLK3	5.98E-12	1.501881863	2.832118956
B3GALT4	0.004292946	-1.229998138	0.426317996
KIFC1	5.31E-22	-1.456351617	0.364413518
SUV39H1	6.61E-09	-1.330747758	0.397562129
TMEM40	4.00E-11	2.992028186	7.955916781
CALCOCO1	1.45E-20	1.353469364	2.555258707
MYMX	0.001649928	1.232793049	2.3502155
ZNF469	2.26E-12	2.900274308	7.465683289

AMIGO1	0.000199706	1.211880548	2.316393812
COX18	2.57E-05	-1.016876889	0.494184995
RTN4RL2	0.001352236	-1.083131862	0.472003066
SEMA3G	3.31E-18	2.071645419	4.203658348
PROCR	6.26E-12	1.23759823	2.358056408
GIPR	0.003695755	-1.441277975	0.368240963
OPN3	0.006210261	-1.704057702	0.306921645
YEATS4	1.10E-07	-1.092621845	0.468908441
ESPL1	3.63E-18	-1.283068619	0.410920549
PYGM	2.02E-27	-1.924824385	0.263372316
GABBR2	2.18E-16	3.899435068	14.92268328
NAAA	8.56E-05	-1.231995349	0.425728226
TYRP1	2.46E-11	1.650285207	3.138956872
CRIP2	1.00E-09	1.099830413	2.143294968
SLC25A10	6.03E-10	-1.06882339	0.476707626
CAMK1D	0.000708362	-1.213183662	0.43131576
MLKL	0.00444668	-1.041884745	0.485692548
PCDHGA12	1.85E-06	1.454004411	2.739674337
STPG3	0.003974066	-1.279504213	0.411937048
LIN9	2.50E-08	-1.112376901	0.462531363
AC099489.1	0.008314593	1.009867784	2.013726543
ZMAT3	1.24E-35	1.668543199	3.178934297
TNFRSF10D	1.61E-33	1.559993122	2.948524378
PCDHB11	2.55E-07	1.19595858	2.290970021
ZSCAN30	4.36E-18	1.427795206	2.690352489
HMMR	7.28E-21	-1.481819308	0.358037025
ZNF383	0.003963288	2.652965431	6.289587629
CDC6	2.94E-13	-1.123430924	0.45900096
CDKN3	1.01E-08	-1.414874975	0.375042247
HS1BP3	7.83E-23	1.33834236	2.528606178
HIRIP3	5.39E-07	-1.161004509	0.447201053
TBX6	0.001166815	-1.065134995	0.477927936
FAM57B	0.007666988	-1.035873375	0.487720536
SULF2	1.11E-87	4.061935747	16.70184698
BLM	7.30E-16	-1.491643916	0.355607112
AC006059.2	7.39E-57	4.33623383	20.19930612
HRC	3.85E-13	-2.137264181	0.227310435
SOX7	0.0017107	1.02926128	2.040978917
TPM4	9.82E-24	1.128185849	2.185837042
ATAD5	1.21E-17	-1.580989115	0.334252646
TRIM7	1.93E-06	-1.601778924	0.329470472
INSYN2	1.28E-23	3.229238998	9.377731661
SUSD2	5.58E-08	1.774336391	3.420806242
RGL1	8.50E-10	1.082263568	2.117355577
PAQR9	0.002224845	-1.167134028	0.445305079
SLC4A11	3.57E-12	1.110080627	2.158577105
GLTP	1.80E-07	1.025799049	2.036086776
MIB2	5.86E-23	1.527042637	2.881944669
NXPH3	1.98E-07	-1.739449176	0.299483998

HIST1H2BJ	4.16E-06	1.831663115	3.559471662
PBXIP1	6.87E-29	1.580151039	2.990011512
ARHGEF39	0.000145696	-1.140006777	0.453757446
ZNF296	2.66E-20	1.937439064	3.830251338
POLA1	2.21E-10	-1.15182384	0.450055915
CEP135	5.07E-06	-1.046706555	0.484071964
CEP170B	4.40E-26	1.484588736	2.798373894
PRAMEF5	1.54E-16	4.102008936	17.17227095
GPR137C	9.69E-06	-1.303253298	0.40521141
FAM162A	8.00E-10	-1.016895036	0.494178779
BMP1	1.02E-10	1.157008039	2.229944863
ANK1	1.53E-62	3.14337478	8.835885844
GLDC	1.68E-21	1.303459293	2.468199984
SMAD3	5.67E-33	1.841059222	3.582729748
BTG1	4.36E-08	1.02420144	2.033833306
KIAA1211L	0.000731827	1.323489352	2.502706916
FILIP1L	5.44E-07	1.50537592	2.838986364
DCK	2.37E-08	-1.138802481	0.45413638
TP53I3	3.91E-104	2.582949336	5.991633323
TC2N	1.93E-08	2.552162154	5.865126212
LDLRAD1	3.73E-08	3.678590384	12.80460092
PRAMEF7	1.26E-24	Inf	#VALUE!
PIK3R5	0.001194018	-1.184985503	0.439828958
AC233992.2	3.18E-08	1.935572667	3.825299393
NCCRP1	5.59E-07	-2.146644556	0.225837261
ITM2A	0.002457383	1.320377975	2.497315289
LEUTX	8.49E-26	4.779913912	27.47245458
TJP2	1.33E-06	-1.290312067	0.408862579
C1orf112	3.80E-05	-1.001253015	0.499565927
PADI3	0.001077391	1.479597126	2.788708475
AS3MT	0.000146852	-1.065444197	0.477825516
ZMAT4	0.00082904	1.53385884	2.895593012
SKA1	1.06E-08	-1.568629641	0.337128467
ANKRA2	1.85E-16	1.521365926	2.870627084
SAPCD2	2.49E-11	-1.173480882	0.443350349
STIL	0.009847376	-1.134150891	0.455602986
SCRIB	1.84E-20	1.174277169	2.256797807
C16orf96	0.004228888	1.1804818	2.266524568
CABCOCO1	0.000277738	-2.277104256	0.206311442
SMC2	8.04E-16	-1.219421411	0.429454915
HIST2H4B	0.001150643	1.145506684	2.212238123
FAM72D	5.84E-08	-1.467981663	0.361487668
RMI2	8.86E-10	-1.453209111	0.365208156
MIS18BP1	1.56E-11	-1.183351647	0.440327347
TIFA	0.001712228	-1.095619692	0.467935085
CDIP1	1.55E-20	1.289290472	2.444078244
FRG2C	3.70E-36	6.053908142	66.43668306
PIF1	2.24E-10	-1.498157365	0.354005244
ISY1-RAB43	2.62E-17	Inf	#VALUE!

RAD51B	0.000645081	-1.215954818	0.430488076
ITGAM	1.46E-05	1.397417713	2.634296458
ISM2	0.002310983	-1.158969954	0.447832162
WFIKKN1	0.003055804	-1.180805233	0.441105229
TNFSF9	9.08E-16	1.579293672	2.98823513
GXYLT1	6.16E-15	1.176886296	2.260882939
KANK3	1.19E-07	2.176563755	4.520755067
PALLD	3.61E-14	1.039648598	2.055726872
PLA2G4B	2.22E-09	-2.205876791	0.216752901
TUBA1B	5.77E-23	-1.028940219	0.490070014
PORCN	6.76E-13	1.49737363	2.823282767
EPHA2	2.01E-17	1.039676105	2.055766067
ORC6	6.03E-13	-1.41927741	0.373899537
CCNE2	1.85E-06	-1.486728358	0.356820805
PLEKHG1	8.20E-16	3.192338935	9.140917216
E2F2	6.28E-10	-1.362957168	0.38878456
TTYH3	1.83E-31	1.476783718	2.783275498
PRPH	0.003044751	-1.276567315	0.412776483
FBXO5	1.91E-08	-1.109733618	0.463379582
DPYSL4	4.60E-62	2.537513025	5.805873043
FBXL12	2.53E-05	1.162825131	2.238954377
TREML1	0.000187971	1.545817868	2.919695403
CDT1	2.00E-12	-1.065346953	0.477857725
ABCA12	1.80E-21	3.770448901	13.64640375
XKR5	5.33E-06	-1.393589909	0.380616521
SNX29	2.10E-08	1.159900366	2.23441996
EFNB1	9.01E-37	2.148361063	4.433238757
GINS3	0.000203042	-1.002056138	0.499287904
BAIAP3	0.008023224	-1.105368738	0.464783662
MVP	2.82E-22	1.410183018	2.657708759
ARMH1	0.009124784	1.020264362	2.028290593
TAF11L11	4.04E-40	3.763041858	13.57652033
PIMREG	2.10E-10	-1.460297261	0.363418241
SSU72P7	9.14E-69	5.779251523	54.91968795
CYSRT1	5.40E-06	1.312878404	2.484367162
MUC20	0.000887494	1.161484456	2.236874717
FMN1	0.00160319	1.072241413	2.102697643
SLC1A4	1.90E-05	-1.219785631	0.42934651
EMILIN2	0.001750665	1.447252195	2.726881855
FANCD2	1.42E-20	-1.435613192	0.369689714
CPHXL	3.82E-22	6.165076312	71.75842456
SYNPO2L	0.003904859	1.250090598	2.378563594
CENPH	1.11E-09	-1.545586058	0.342556518
ARL2	1.01E-13	-1.167908847	0.445065986
SNCB	0.003933391	-1.473808769	0.360030549
COL4A6	1.94E-17	1.747627894	3.358059734
ANLN	2.50E-24	-1.358720115	0.389928061
NDC80	1.20E-16	-1.686320082	0.310718472
CABYR	5.46E-12	1.570644459	2.970373725

MASTL	2.72E-14	-1.298762179	0.406474801
PSMC3IP	1.32E-05	-1.115630844	0.461489317
ARC	1.14E-27	3.085290033	8.487207993
SIRT2	1.93E-22	1.553578817	2.935444169
FER1L6	1.37E-19	4.129830227	17.50663896
CDCA5	1.96E-15	-1.297048776	0.406957834
NUDT1	1.96E-05	-1.143253182	0.452737533
CDCA3	1.80E-12	-1.274657578	0.413323249
SHISA7	0.000471103	-1.411817899	0.375837806
GPHA2	9.73E-05	-1.550196011	0.341463668
MCM7	1.16E-19	-1.133335269	0.455860633
MYBL1	3.27E-07	-1.174654447	0.442989851
MICALL1	1.93E-31	1.522604532	2.87309268
NUPR1	6.54E-07	1.800086616	3.482411323
PRR35	0.000992062	-1.501576595	0.353167234
TOP2A	3.84E-38	-1.506695352	0.351916399
KIF2C	6.21E-28	-1.592427979	0.331612897
KIF4A	2.26E-19	-1.468368365	0.361390788
RASSF5	0.007664625	-1.08546582	0.471240088
CKAP2L	6.02E-15	-1.70420304	0.306890727
INCENP	2.52E-18	-1.199929943	0.435296419
KNTC1	1.77E-24	-1.449333468	0.366190567
MMD	0.002962024	-1.022949663	0.492109181
MND1	1.64E-10	-1.620523303	0.325217478
TP53I11	1.54E-37	2.307574917	4.950502307
CD302	2.71E-05	-1.273960034	0.41352314
ZDHHC22	1.97E-24	5.69623545	51.8486834
BBS1	1.37E-07	1.378021656	2.599117139
RAD54L	4.20E-11	-1.227153896	0.427159302
COL5A1	2.38E-54	4.795700277	27.77471642
PPIH	2.45E-06	-1.063247477	0.478553632
DNAH6	7.54E-09	-2.369572254	0.193502988
IGFN1	7.60E-13	-1.366030985	0.387957095
C2CD4C	1.20E-07	-1.619565709	0.325433413
KCNC4	1.73E-07	1.467537011	2.765493615
MUC19	1.96E-18	4.41437297	21.32350911
APOBEC3B	3.48E-13	-1.333659572	0.396760533
RADX	9.07E-08	-1.215320759	0.430677315
LRG1	0.000765745	-1.387888346	0.382123702
BIRC3	2.15E-05	-1.231039498	0.426010384
TMSB15A	7.71E-06	-1.496170143	0.3544932
FGFBP3	9.11E-09	-1.078032875	0.473674241
TSPEAR	3.98E-05	1.343878423	2.538327855
NECTIN4	5.67E-33	3.371002798	10.34601152
TTC39B	0.000554517	-1.231363059	0.425914851
CEP152	1.26E-13	-1.353040614	0.391466128
CSNK1G1	0.001151646	1.100114784	2.143717477
HSPA1A	0.00990359	4.873033688	29.30416224
JAM2	0.002075642	-1.388609197	0.38193282

HIST1H2BG	0.003711342	1.44509024	2.722798537
SLC12A8	0.000224811	2.060752647	4.172039009
UCHL5	1.25E-12	-1.168903222	0.444759331
LAT2	0.002237466	1.281423503	2.430787037
CENPU	1.93E-09	-1.26572716	0.415889694
CYP1A1	0.000282975	-1.291301419	0.408582291
COQ8A	9.81E-27	1.54102337	2.910008505
CSF1	8.31E-31	1.939127381	3.834736323
SCN1B	0.004846364	-1.165023705	0.445956932
UBASH3B	1.94E-29	3.249019704	9.507194686
CYGB	4.56E-16	2.045452837	4.128028229
MBD3L2B	4.96E-61	5.485834174	44.81265112
XRCC2	1.38E-12	-1.386577976	0.382470935
IP6K3	1.30E-18	2.342983572	5.073507824
RIMKLA	8.16E-10	-1.576313998	0.335337563
EXO1	5.89E-15	-1.383514521	0.383283947
RAB5B	1.48E-35	2.276473174	4.844921108
NEIL3	1.11E-10	-1.833835463	0.280517861
FBXW7	9.84E-11	1.037158304	2.052181461
PRSS23	0.000332096	1.073671305	2.104782713
NGFR	3.87E-35	1.920715965	3.78610905
P2RX3	0.000143007	-1.966985303	0.255786973
TLX2	4.69E-10	1.992100993	3.978159149
CYFIP2	5.05E-77	2.518876888	5.731357497
NCAPH	1.69E-15	-1.318407448	0.400977323
RFLNB	6.03E-07	-1.205663264	0.433569968
TRIM49C	3.81E-71	5.890875918	59.3376513
TAF5	2.44E-06	-1.093607114	0.468588316
ABHD3	1.06E-06	1.112613325	2.162369885
DSCC1	2.63E-10	-1.243871908	0.422237931
PATL2	0.001892888	1.187387693	2.277399978
SLC12A4	1.91E-15	1.068888372	2.097816332
HYAL1	0.000387489	-1.117887632	0.46076798
SYNC	0.001263987	1.152364723	2.22277932
NT5M	0.003240404	-1.180016945	0.441346314
RDM1	4.69E-08	-1.914255406	0.265308829
GALNT4	2.76E-15	1.164134746	2.240987724
BLOC1S2	2.80E-12	1.209409758	2.312430102
CARMIL1	1.18E-14	3.14941835	8.872977748
PLXDC1	1.02E-15	2.123954103	4.358869775
MZT1	6.95E-07	-1.142500278	0.452973866
FCGBP	0.00016703	1.152954214	2.223687742
CEL	4.12E-06	1.317724328	2.492726031
COL17A1	1.16E-59	4.634206287	24.83333793
CEACAM1	5.94E-21	2.727778924	6.62435011
GTPBP10	1.63E-05	1.063378679	2.08981999
ATP8B4	0.000171917	2.918911181	7.562751322
NSG1	1.26E-27	4.802182119	27.89978538
TEX19	2.15E-05	-1.094789808	0.468204333

EPPK1	1.22E-10	1.744156842	3.349990124
NDC1	2.89E-12	-1.021928113	0.492457759
TAF11L13	9.86E-18	4.143580751	17.67429484
LAMC3	2.44E-39	2.467730795	5.531730205
PCDHGB6	6.09E-12	1.68744365	3.220854859
SLC4A7	1.26E-12	-1.06605345	0.477623773
ISCU	1.31E-17	1.285927683	2.438387957
BARD1	1.26E-08	-1.295732207	0.407329383
UBE2T	1.27E-15	-1.441111579	0.368283437
IL22RA1	3.21E-26	4.01862991	16.20795209
STAT3	8.32E-15	1.124670374	2.180517205
MBD3L4	2.25E-57	5.903526684	59.86026181
PCLAF	2.06E-10	-1.058651332	0.480080641
ZFYVE1	7.16E-11	1.114362474	2.164993171
TNNI1	0.000106928	-1.462785498	0.362791988
ZNF561	1.48E-28	1.625063945	3.084558366
TROAP	1.36E-16	-1.483713658	0.357567208
RHOB	9.68E-39	1.596227355	3.023516297
MAST4	6.44E-12	2.760529722	6.776450186
USP1	5.26E-11	-1.013977501	0.495179158
MCM2	8.66E-18	-1.084618523	0.47151693
ZBTB5	1.26E-52	1.930043759	3.810667575
KLHL30	0.000641052	1.190111452	2.281703693
KCNJ11	0.001958625	1.189880951	2.281339171
SLC34A2	7.50E-253	6.269086202	77.12283616
RNMT	6.95E-07	1.279734765	2.427943358
S100B	0.002083229	-1.346954282	0.393121104
AC068831.7	3.53E-11	-1.116587144	0.461183517
ACER2	8.28E-34	2.506178121	5.681130807
HERC5	0.001246742	1.028357253	2.039700393
CELF2	2.83E-16	4.132689731	17.54137253
E2F1	4.15E-09	-1.209236743	0.432497368
FEZ1	1.36E-18	2.653453046	6.291713799
SCUBE1	8.28E-06	-2.116107514	0.230668432
HHATL	7.88E-33	4.606414403	24.35953018
SFN	2.40E-39	2.493401851	5.631041763
PRAMEF4	2.50E-19	5.069773409	33.58565847
TMEFF1	2.99E-06	-1.17449799	0.443037895
CCNA1	3.09E-11	4.569776932	23.74870485
RAB27B	3.23E-06	-2.073353798	0.237606499
CHAC2	0.001007218	-1.019420488	0.49331447
RAD51AP1	1.96E-12	-1.477656797	0.359071537
ZNF670-ZNF695	0.002912245	-1.40297131	0.378149519
AGT	2.57E-05	-1.51803933	0.349160114
TTK	6.00E-19	-1.56062397	0.33900443
VASN	4.72E-09	1.440445892	2.714047352
ERBB3	6.81E-10	-1.826886234	0.28187233
KLHL21	1.01E-13	1.114174293	2.164710793
CLCA2	1.05E-67	3.733431571	13.30071199

LAMP3	1.30E-06	1.747766802	3.358383077
TAF3	2.25E-31	1.808259742	3.502195795
HMCN2	1.47E-06	2.234486914	4.705953005
CKS1B	3.19E-17	-1.200905535	0.435002159
IFIT1	5.98E-12	1.065862435	2.09342094
HIST1H3E	6.18E-05	1.215819323	2.322726558
CCNK	4.34E-19	1.173707471	2.255906809
PLK4	5.09E-18	-1.510907892	0.350890333
PRAMEF8	9.11E-28	Inf	#VALUE!
IQCD	1.74E-05	-1.555740537	0.340153883
POLA2	3.71E-13	-1.104853641	0.464949637
CENPM	7.06E-06	-1.098554946	0.466984009
ANGPTL6	0.003044751	-1.236029584	0.424539417
COL24A1	1.75E-15	4.428755133	21.53714532
SSU72P8	1.48E-11	4.516702997	22.89091135
MTFR2	1.20E-06	-1.383588488	0.383264296
HES2	2.58E-20	2.564600405	5.915911233
ASCC3	1.52E-15	1.013799906	2.019222521
TRIM49D1	9.01E-37	5.079842485	33.82088449
HOXA5	0.002699627	1.060581049	2.085771402
PRR20G	4.19E-21	6.332347437	80.57986244
SELENOF	0.003767094	-1.645016318	0.319742779
LTBP2	4.26E-08	1.24038119	2.362609491
TEAD3	0.000469765	1.325076962	2.505462531
SUSD6	1.28E-25	1.700623585	3.250414228
CARD14	4.57E-07	1.411660903	2.660432689
SLC16A3	1.29E-07	-1.012387533	0.495725187
LRP11	2.14E-05	-1.124335132	0.458713372
CT45A1	0.000131342	1.627202687	3.0891345
SENP3-EIF4A1	0.004819689	1.041541965	2.058426542
SNX24	3.09E-16	-1.932385998	0.261995512
PRKAB2	3.02E-15	1.03837813	2.053917352
C5orf34	3.63E-08	-1.483013704	0.357740732
YPEL5	1.16E-08	1.133403892	2.193757249
SPC25	1.71E-10	-1.620983145	0.325113835
RECQL4	9.64E-05	-1.027189331	0.490665136
DHRS3	2.38E-10	2.153205691	4.448150775
LRRC38	1.62E-27	6.320930352	79.94469252
DRAXIN	4.04E-57	4.725031771	26.44699259
PAPPA	0.000469203	1.178861504	2.263980456
PLK2	2.55E-10	1.581532794	2.992876596
CDC45	2.47E-14	-1.333824652	0.396715136
MDM2	1.93E-48	1.782817666	3.440975609
CDC25B	5.31E-11	-1.140930768	0.453466925
OTULINL	8.05E-16	3.322686523	10.0052584
CDC20	1.48E-14	-1.147036153	0.451551939
NCAPG2	1.16E-19	-1.433461401	0.37024152
SIAE	0.002275532	1.044431541	2.062553499
METRNL	1.21E-05	1.931455436	3.814398135

ACHE	4.67E-26	2.158664748	4.465014152
GNG2	0.005814099	-1.268531032	0.415082199
JAG2	9.35E-14	1.111551207	2.160778525
POLE2	7.42E-10	-1.450132287	0.365987864
MCM5	2.57E-17	-1.116182923	0.461312752
BIK	8.45E-10	2.686918836	6.439366821
PXYLP1	0.001126051	-1.674887855	0.313190454
FAM83H	4.21E-24	1.408503519	2.654616615
RFPL4B	1.47E-136	5.27988535	38.8511487
SDC3	2.45E-12	1.045856482	2.064591677
ECT2	3.26E-13	-1.072453054	0.475509789
TRIM74	0.003191896	1.328820189	2.511971661
ESCO2	8.04E-12	-1.541303499	0.343574889
TOM1L2	2.31E-11	1.070113474	2.099598503
RRM2B	4.98E-13	1.046395173	2.065362723
ZNF367	6.68E-09	-1.572322704	0.336266577
FRMD1	1.91E-06	1.719737752	3.293765286
FDXR	1.02E-41	1.738412664	3.336678453
DOCK8	1.94E-15	1.420702921	2.677159178
PACSIN1	4.87E-07	-1.620615169	0.32519677
TNFRSF10B	1.90E-16	1.035187631	2.049380163
HLA-DOA	3.89E-06	1.351544619	2.551851928
TNNT3	0.000190958	1.2868073	2.439875106
PHLDA3	2.42E-17	1.263520509	2.400808794
LHX4	1.77E-11	1.370211304	2.585084257
C4orf47	0.000252363	-1.492475189	0.355402272
CNIH2	9.38E-06	-1.189558182	0.438437109
ANKRD65	0.000137475	1.454618892	2.740841482
HRNR	0.00012395	1.148814325	2.2173159
CFAP74	0.007040716	1.06444185	2.091360617
GJD3	9.04E-14	2.020441983	4.057080653
CENPE	1.25E-27	-1.462784816	0.36279216
POLQ	3.31E-18	-1.528959941	0.346527093
TMEM229B	1.50E-06	1.494293398	2.817261337
TRIM35	1.82E-14	1.378572283	2.600109323
FAM92B	0.000193953	1.188748001	2.279548336
PRIM1	3.18E-09	-1.223876429	0.428130811
IMPA2	1.77E-07	-1.172590682	0.443623999
CLSTN2	1.17E-08	2.480859645	5.582299947
FBXO36	0.000346333	-1.126678872	0.457968771
HEG1	5.89E-08	1.682486193	3.209806198
CUTC	2.76E-07	-1.357957252	0.3901343
TRAF4	1.46E-28	1.578938274	2.98749909
COL18A1	2.44E-15	1.229539863	2.344921884
MBD3L3	1.87E-63	5.656966905	50.45645366

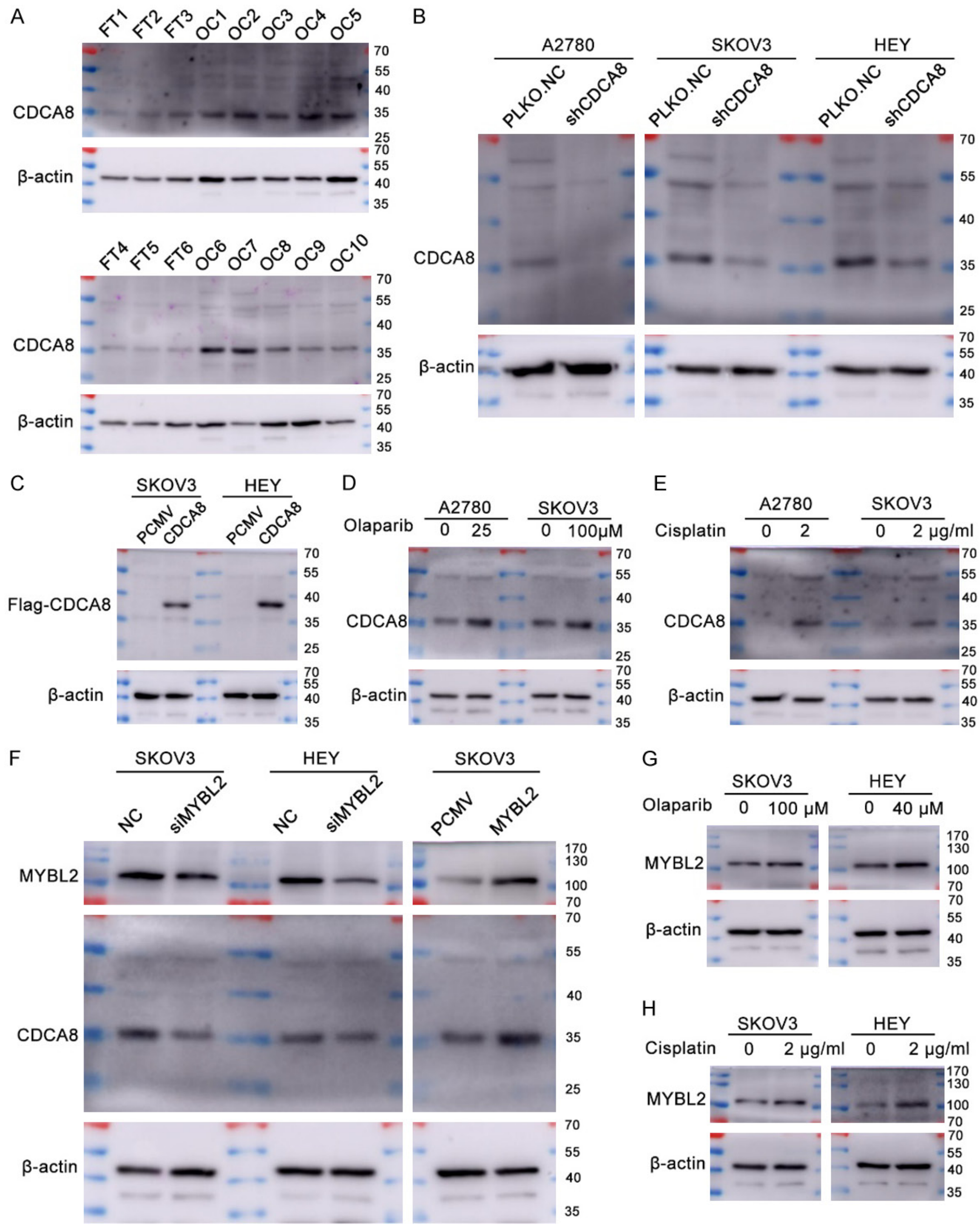

Figure S2. Original, full-length blot images. (A) Original blot images of **Figure 1T**, the protein level of CDCA8 in HGSOC and FT tissues. (B) Original blot images of **Figure 2A**, the CDCA8 level in ovarian cancer cells after transfection with PLKO.NC or shCDCA8. (C) Original blot images of **Figure 2I**, the expression of CDCA8 in SKOV3 and HEY cells after transfection with PCMV or CDCA8. (D) Original blot images of **Figure 3B**, the CDCA8 expression in A2780 and SKOV3 cells after olaparib treatment. (E) Original blot images of **Figure 3E**, the CDCA8 protein level in A2780 and SKOV3 cells following cisplatin treatment. (F) Original blot images of **Figure 6B**, the protein level of CDCA8 and MYBL2 in SKOV3 and HEY cells after transfecting with NC, siMYBL2, PCMV or MYBL2 for 48 h. (G) Original blot images of **Figure 8A**, the MYBL2 level in HEY and SKOV3 cells after treating with olaparib. (H) Original blot images of **Figure 8D**, the MYBL2 protein level in HEY and SKOV3 cells following cisplatin treatment.